Chemical Geology 610 (2022) 121090

Contents lists available at ScienceDirect

Chemical Geology

journal homepage: www.elsevier.com/locate/chemgeo

Colloidal associations of major and trace elements in the snow pack across a 2800-km south-north gradient of western Siberia

Ivan V. Krickov [a], Artem G. Lim [a], Sergey N. Vorobyev [a], Vladimir P. Shevchenko [b], Oleg S. Pokrovsky [c,d,*]

[a] BIO-GEO-CLIM Laboratory, Tomsk State University, Lenina av., 36, Tomsk, Russia
[b] Shirshov Institute of Oceanology, Russian Academy of Sciences, Nakhimovsky prospect, 36, Moscow, Russia
[c] Geoscience and Environment Toulouse (GET), UMR 5563 CNRS University of Toulouse, 14 Avenue Edouard Belin, 31400 Toulouse, France
[d] N. Laverov Federal Center for Integrated Arctic Research of the Ural Branch of the Russian Academy of Sciences (FECIAR UrB RAS), Arkhangelsk, Russia

ARTICLE INFO

Editor: Dr Don Porcelli

Keywords:
Snow
Colloids
Carbon
Trace element
River
Arctic

ABSTRACT

Colloidal (size 1 nm to 1 μm) transport of major and trace elements, notably micronutrients and low-solubility geochemical tracers, is a ubiquitous and well-established feature for all surface and soil waters in boreal and subarctic regions. However, little is known on the colloidal associations of organic carbon (OC) and major and trace elements in atmospheric precipitation such as snow. This is despite significant efforts devoted to distinguishing the soluble and particulate transport of trace metals and contaminants by atmospheric aerosols. To acquire a *snap-shot* of major and trace element size fractionation in the snow cover of western Siberia, we sampled snow cores integrated over the entire depth (0–50 cm until bottom) across a sizable (2800 km) south - north transect in the Ob River watershed (western Siberia). A number of trace metal pollutants (Cr, Ni, Zn, Cd) exhibited significant linkage, pronounced over the first 20 km, to sources of local pollution. Some elements (P, Mn, Zn, Ba) also demonstrated an increase in their colloidal fraction in the proximity of pollution centers, possibly reflecting input from industrial centers and gas flares.

Following centrifuginal ultrafiltration, we analyzed total dissolved (< 0.22 μm), two colloidal (high molecular weight, $HMW_{50\ kDa-\ 0.22\ \mu m}$; medium molecular weight $MMW_{3\ kDa-\ 50\ kDa}$) and low molecular weight (LMW < 3 kDa) fractions in the melted snow for all major and trace elements. We discovered sizable (20 to 70%) proportion of some major (Ca, SO_4) and many trace (Fe, Y, Zn, Sb, La, Ce, Yb, Pb) elements in the colloidal (3 kDa - 0.22 μm) form, without significant link to latitude, type of biome, or the concentration of possible colloidal carrier (DOC, Fe, Al, Ca, SO_4). The origin of snow water colloids in snow can be hypothesized to stem from solute freezing on lake surfaces (Fe, OC), frost flowers of the Arctic ice (Ca, SO_4), clays dispersion (Al, Si) and sulphur dioxide oxidation particles (SO_4, oxyanions). Via hydrochemical mass balance calculations, we demonstrate an overwhelming impact of snow melt on spring-time riverine export of Cd, Pb, Zn, As, Sb and Cs. These preliminary results call for further studies of atmospheric colloids including those originating from rainwater.

1. Introduction

A rising interest on the geochemistry of surface water, soil and vegetation in Arctic and subarctic regions stems from the pivotal role of these regions in planetray-scale carbon regulation, notably nutrient and metal exchange between the terrestrial, oceanic and atmospheric sources (Ciais et al., 2013; Tamocai et al., 2009; Schuur et al., 2015). However, in contrast to a relatively good understanding of major and trace element concentrations and fluxes in inland waters in high latitude regions, the atmospheric input of elements from rain water and snow melt remain extremely poorly constrained. This limited understanding is mostly due to restricted access to remote areas all year long, sizable variations in atmospheric precipitates over the territory and difficulties in sampling/handling of contamination-vulnerable atmospheric precipitates. Due to these reasons, areal transect-like studies of snow cover remain the most efficient and representative way of assessing integral

* Corresponding author at: Geoscience and Environment Toulouse (GET), UMR 5563 CNRS University of Toulouse, 14 Avenue Edouard Belin, 31400 Toulouse, France.
E-mail address: oleg.pokrovsky@get.omp.eu (O.S. Pokrovsky).

https://doi.org/10.1016/j.chemgeo.2022.121090
Received 31 May 2022; Received in revised form 7 August 2022; Accepted 28 August 2022
Available online 1 September 2022

(over full depth of the snow cover, corresponding to the entire winter season) precipitation of the dissolved and particulate components of atmospheric aerosols (Tranter et al., 1986; Shaw et al., 1993; Colin et al., 1997; Shevchenko et al., 2017). Over recent years, a sizable number of studies were devoted to the chemical composition of winter time aerosols (especially particulate fraction) in Arctic and subarctic regions (Conca et al., 2019, 2021; Becagli et al., 2020; Bazzano et al., 2016; Koziol et al., 2021). The majority of these works represented either small regional studies of background concentrations or were devoted to tracing sources of local aerosol pollution (Moskovchenko and Babushkin, 2012; Moskovchenko et al., 2021; Pozhitkov et al., 2020; Salo et al., 2016; Shevchenko et al., 2016; Talovskaya et al., 2014; Topchaya et al., 2012; Vlasov et al., 2020; Walker et al., 2003; Xu et al., 2016). The dissolved (< 0.45 μm or < 0.22 μm) fraction of melted snow was extensively investigated in European subarctic regions (de Caritat et al., 1998; Chekushin et al., 1998; Kashulina et al., 2014; de Caritat et al., 1997, 1998, de Caritat et al., 2005; Reimann et al., 1996; Reinosdotter and Viklander, 2005) and there were numerous studies on trace element geochemistry of the snow cover in high altitude zones of Asia and northern China (Dong et al., 2015; Kang et al., 2007; Lee et al., 2008; Wang et al., 2015; Wei et al., 2019; Li et al., 2020), South America (Cereceda-Balic et al., 2012), glaciers in Greenland (Barbante et al., 2003; Boutron et al., 2011; Candelone et al., 1996; Lai et al., 2017), Spitzbergen (Kozak et al., 2015), and Alaskan and Canadian High Arctic areas (Barrie and Vet, 1984; Douglas and Sturm, 2004; Garbarino et al., 2002; Krachler et al., 2005; Snyder-Conn et al., 1997). However, the majority of these works dealt with rather limited geographical coverage that did not allow assessing global river watershed-scale influence of the snowfall on chemical element fluxes in surface waters. Only in the Western Siberian Lowland (WSL), has a sizable (1700–2800 km) latitudinal gradient been covered over two sampling campaigns (Shevchenko et al., 2017; Krickov et al., 2022). However, the first campaign dealt only with the surface (0–5 cm) snow layer while the second campaign reported only a few heavy metals in the dissolved (< 0.22 μm) fraction.

A typical feature of high latitude regions is a relatively high concentration of organic matter which provokes enrichment of all inland waters in typically low mobility trace metals. Organic-rich soils and sediments, dissolved (< 0.22 or 0.45 μm) organic matter, and Fe / Al oxy (hydr)oxides are the main vectors of trace metal transport in rivers, lakes and soil porewaters of high latitude regions (Pokrovsky et al., 2016a, 2016b; Cuss et al., 2018; Raudina et al., 2021). Trace elements and DOM are usually present in the so-called colloidal fraction, having a size between 1 nm and 1 μm [or operationally defined as 1–3 kDa and 0.22–0.45 μm]. These groups of colloids have been evidenced to dominate surface waters of Arctic and subarctic regions across boreal and subarctic zones from Northern Europe (Ilina et al., 2016; Lyvén et al., 2003; Pokrovsky et al., 2012, 2010; Pokrovsky and Schott, 2002) to Central Siberia (Bagard et al., 2011; Pokrovsky et al., 2016a), Alaska (Stolpe et al., 2013) and Canada (Cuss et al., 2018). The colloidal status of DOM and related metals is a fairly well established feature of all humic (organic-rich) surface waters (Shirokova et al., 2013; Loiko et al., 2017; Pokrovsky et al., 2014), rivers (Krickov et al., 2019), peat porewaters (Raudina et al., 2021) and ice (Lim et al., 2022) of the Western Siberia Lowland. However, to the best of our knowledge, any information on colloidal associations of trace metals in the snow, notably from Siberian peatlands, is absent. The only exception is a recent work from Jensen et al. (2021) who demonstrated that Arctic snow contained higher concentrations of colloidal metals (Fe, Zn) relative to the seawater.

Information on snow colloids is of fundamental importance for assessing the origin and pathways of trace metal in snow. This information might also have crucial influence on our understanding of climate warming-induced future changes in atmospheric precipitation and surface water distribution in Arctic and subarctic regions - given that the contribution of liquid atmospheric aerosols and soluble forms of some metals and metalloids is comparable to or may even exceed the export of these elements by Arctic rivers (Shevchenko et al., 2017; Krickov et al., 2022). In the present work, we used the unique geographical position, the WSL being the largest peatland in the world, to assess the colloidal associations of major and trace elements in the snowpack across a sizable south - north gradient within the Ob River watershed. Further, the Ob River watershed encompasses both boreal and subarctic biomes (southern and northern taiga, forest-tundra and southern tundra). Via sampling of snow cores integrated over the entire depth (0–50 cm to bottom) with unprecedented geographical coverage of >2700 km in a latitudinal transect, we focused on the following objectives: (1) estimate the average concentrations of colloidal forms of major and trace elements (TE) in the snowpack of western Siberia; (2) quantify the distribution of TE between different colloidal fractions; (3) test the role of latitude (south-north profile) and physio-geographic zones on colloidal proportions of elements in snow; (4) assess the chemical nature of major colloidal carriers of TE, and finally (5) quantify the contribution of snow precipitation to element export as total dissolved and low molecular form by the WSL rivers.

2. Study site and methods

2.1. Geographical setting and snow sampling

We used existing road infrastructure to sample a sizable (2800 km) latitudinal transect of the WSL. Snow cores were collected along a south → north gradient, from the vicinity of the Barnaul city (forest-steppe zone) to the Ob estuary (tundra zone) from February 8 to February 19, 2020. The entire snow cores (50 ± 10 cm long, from surface to the ground, minus the bottom 2–3 cm layer to avoid sampling grass) were collected at 36 locations along the transect. Sampling sites were evenly distributed along the transect (Fig. 1). All sampled points were located >500 m from the nearest road. Note that the traffic density of these temporal (winter, or zimnik) roads in western Siberia is quite low (<10 vehicules per hour).

Snow collection was performed using a clean sampling technique in a protected environment. We used only plastic / PVC equipment and vinyl single-use gloves. First, a pit was dug in the snow with a plastic shovel to examine the representability of the studied location and the evenness of the bottom. Next, a two-person team sampled the snow in a fashion so that no contamination from external surfaces (other than plastic shovel) was possible. The plastic shovel was inserted 2 cm above the ground in order to avoid touching any ground vegetation during sampling. The snow was collected in duplicates via a 10-cm diameter PVC tube which was inserted in the snow till the shovel surface was a few cm above the grass surface to avoid any contamination from plant debris. Prior to sampling, the tube and shovel were “rinsed” several times with fresh snow via insertion into snow cover 1–2 m from the sampling site.

Approximately 5 L of duplicated snow cores were transferred into single-use polyethylene bags, which were doubly closed with a PVC collar. Prior to sampling, polyethylene bags were washed thoroughly with 1 M HCl and abundant MilliQ water in a class A 10,000 clean room. Collected snow samples were transported to the laboratory in the frozen state and processed within 2 weeks of sampling. In the laboratory, snow was melted at ambient temperature and immediately processed for analyses and filtration. The pH and conductivity were measured on unfiltered samples using Hanna portable instruments. Melted snow was filtered through acetate cellulose filters (Millipore, 47 mm diameter) of 0.22 μm pore size. The filtration apparatus was rinsed with large amount of MilliQ water prior to any filtration. The first 200-mL portion of snow water that passed through the filter was used for rinsing the recipient reservoir and discarded. Blanks of MilliQ water from the clean room were also placed in polyethylene bags for the same duration as snow melt ($\langle 3h$) and processed via filtration and ultrafiltration similar to the snow water samples. Filtrates were acidified with double distilled HNO_3 acid and stored in pre-cleaned HDPE tubes for ICP MS analysis. Another

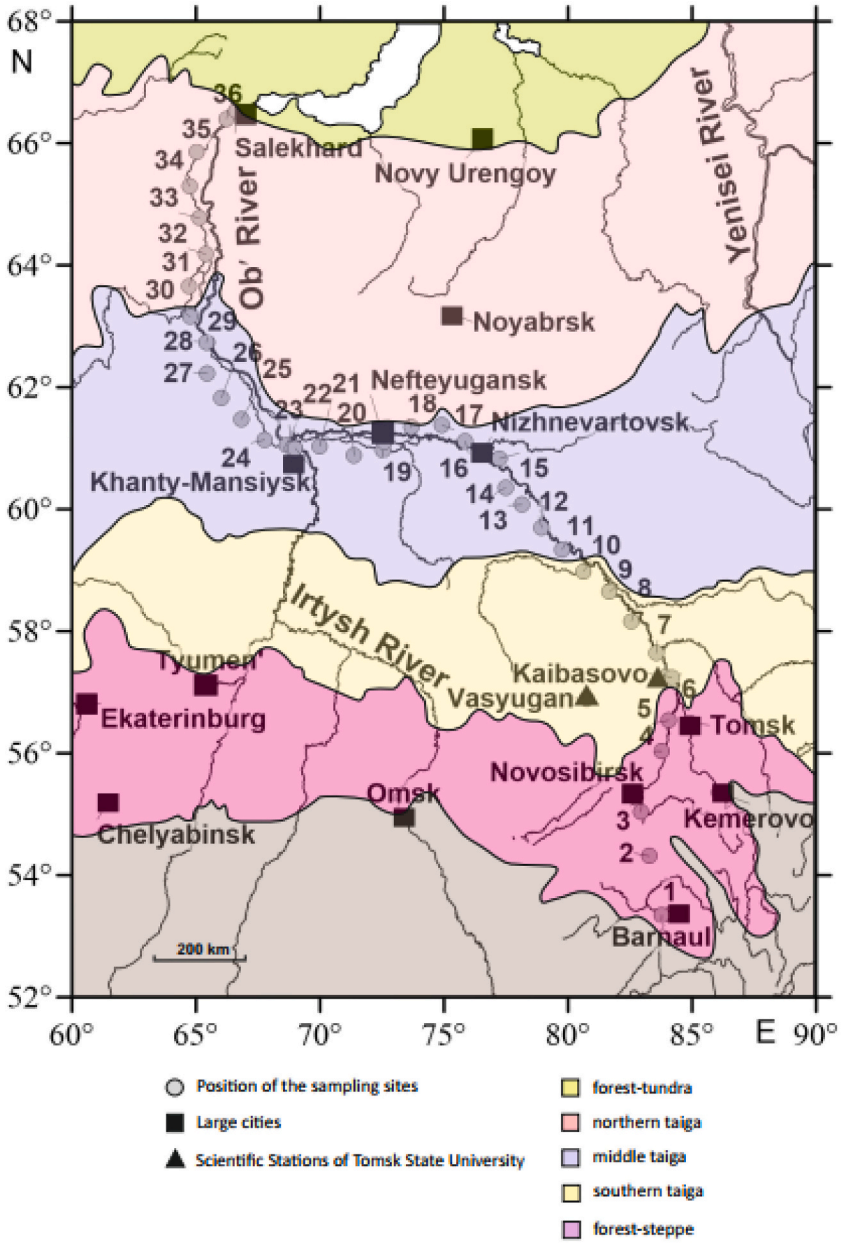

Fig. 1. Studied area of the Western Siberian Lowland (WSL) with physio-geographical zones shown by different colors and sampling points (grey circles) along the winter road.

portion of filtrate was also stored without acidification and used for DOC and anion analyses.

2.2. Size separation and analyses

Filtered (< 0.22 μm) solutions were processed for colloidal size separation using Amicon Ultracell (50 mL) centrifugal/ultrafiltration single-use cartridges. This technique allows for straightforward assessment of the colloidal and truly dissolved pools of elements in natural waters with minimal contamination from the external environment; it is easily performed both in the field and in the laboratory (Banc et al., 2021; Oleinikova et al., 2018, 2017; Raudina et al., 2021). Amicon polypropylene vials were fitted with membranes of 3 kDa and 50 kDa molecular poresize (regenerated cellulose) and were initially treated with 1% HNO_3 and then rinsed 3 times via passing between 50 and 100 mL of MilliQ water through the membrane. The concentration of DOC, major and trace elements in the blanks were a factor of 3 to 10 times lower than the minimal concentrations of these components in the snow water. The first 15-mL portion of sample that was ultrafiltrated through the membrane was discarded. Note that unlike polysulfone ultrafiltration membranes with high surface areas (i.e., Guo et al., 2001) there is no charge separation and preferential retentions or electrostatic repulsion of ions by the 15-mL Amicon ultracentrifugal vials of small filter surface area, in which the retentate is in contact with permeate. At the same time, instead of using integrated ultrafiltrates, rejection of the first portion of ultrafiltrate should eliminate potential sample contamination but may underestimate colloidal abundance if the specific chemical species, notably of inorganic ions, follows the ultrafiltration behavior of macromolecular organic matter (Guo et al., 2000; Guo and Santschi, 2006). Furthermore, one has to keep in mind that size-dependent organic matter, major and trace metal distribution is highly related to sample types and filters/membranes material (Xu and Guo, 2017).

All analytical approaches used in this study followed methods developed for western Siberian surface and atmospheric waters

(Pokrovsky et al., 2016a, 2016b; Shevchenko et al., 2017; Shirokova et al., 2013). In this work we define colloids as entities having sizes between 0.22 μm and 3 kDa. Further, we distinguish a group of high-molecular weight (HMW) ($HMW_{50\ kDa\ -\ 0.22\mu m}$) and medium molecular weight (MMW) ($MMW_{3kDa\ -\ 50\ kDa}$) colloids, and low molecular weight fraction ($LMW_{<\ 3\ kDa}$). Each fraction of filtrate (< 0.22 μm) and ultrafiltrate (< 3 and < 50 kDa) was sub-divided into non-acidified and acidified portions for carbon/anions/pH and trace element measurements, respectively. All samples were preserved via refrigeration 1 month prior to analysis. The pH of the snow water was measured using a combined electrode with an uncertainty of ±0.02 pH units. DOC was analyzed using a Carbon Total Analyzer (Shimadzu TOC VSCN) with an uncertainty better than 3% and a detection limit of 0.1 mg L^{-1}. The DOC concentration in the blank was within the detection limit of the analysis (0.1 ± 0.1 mg L^{-1}). Major anion (Cl, SO_4^{2-}) concentrations were measured by ion chromatography (HPLC, Dionex ICS 2000) with an uncertainty of 2%. International certified samples ION, PERADE, and RAIN were used for validation of the analyses. Major cations (Ca, Mg, Na, K), Si, and ~ 40 trace elements were determined with an Agilent iCap Triple Quad (TQ) ICP MS using both Ar and He modes to diminish interferences. About 3 μg L^{-1} of In and Re were added as internal standards along with 3 various external standards. Detection limits of TE were determined as 3× the blank concentration. The typical uncertainty for elemental concentration measurements ranged from 5 to 10% at 1–1000 μg L^{-1} to 10–20% at 0.001–0.1 μg L^{-1}. The MilliQ field blanks were collected and processed to monitor for any potential contamination introduced by our sampling and handling procedures.

The SLRS-6 (Riverine Water Reference Material for Trace Metals certified by the National Research Council of Canada) was used to check the accuracy and reproducibility of analyses (Yeghicheyan et al., 2019). Only those elements that exhibited good agreement between replicated measurements of SLRS-6 and the certified values (relative difference < 15%) are reported in this study. In addition, we used an in-house standard with low concentrations of major and trace elements, which was prepared via 10-fold dilution of the SLRS-6 Reference Material. Although the 10× diluted SLRS-6 sample was not certified, it was used as a surrogate for assessing elementary concentrations in low-mineralized snow samples. We accepted 20% agreement as satisfactory, between the calculated concentrations of this diluted standard and the actual measured concentrations for all elements.

2.3. Statistical treatment of element concentration data

Solute concentrations at each sampling site were tested for normality using a Shapiro-Wilk test. Because at least a part of the data were not normally distributed, we used non-parametric statistics. Thus, in addion to mean values with s.d., the median and interquartile range (IQR) were used to represent element concentration in each colloidal fraction. We used Spearman pairwise correlations ($p < 0.05$) to assess the link between element concentrations in the 0.22 μm fraction (the main colloidal carriers) and the proportion of TE in the colloidal (3 kDa – 0.22 μm) fraction. Note that measurements of DOC in the <3 kDa fraction often yielded a concentration below or comparative to the quantification limit or the MilliQ blank. Therefore, we used the maximum possible concentration of the DOC in this fraction (0.1 mg L^{-1}) to calculate the proportion of organic carbon in the snow water colloids. The differences in element concentration among main colloidal fractions for a given physio-geographical biome and among different biomes for the same colloidal or LMW fractions were tested using Mann-Whitney test.

Further statistical analysis was used to quantify the relationship between the major and trace element proportion in the colloidal or $LMW_{<\ 3\ kDa}$ fraction and concentration of Fe, Al, or DOC in the <0.22 μm fraction (as main colloidal carriers). We also tested the significance of the impact of latitude and distance to potential object(s) of contamination on the elemental concentration in the 0.22 μm fraction and colloidal fractions.

3. Results

3.1. Average element concentration and proportion of colloids

The concentrations of elements in 3 main fractions (< 3 kDa, < 50 kDa, and < 0.22 μm) separately in four main physio-geographical biomes, and averaged over for the whole territory of western Siberia, are listed in **Table S1** and Table 1. All raw data for each sampled site are provided in the Mendeley database (Pokrovsky et al., 2022). There were significant pairwise Spearman correlations between all elements in the <0.22 μm fraction as well as in the <3 kDa ultrafiltrates (although the latter was less pronounced; **Table S2 A and B**). Examples of the most significant ($p < 0.05$) correlations between some elements and Al or sulfate (as major inorganic colloid constituents, see section 3.2 below) are illustrated in Fig. 2.

Analysis of element size fractionation over the latitudinal gradient demonstrated general independence of the colloid concentration from geographical location, as illustrated in a box plot of the four main physio-geographical biomes (Fig. 3 **A - G** for Mg, Ba, V, As, Mn, Co, Cd, and Pb) and detailed as a function of latitude for Mg, Ba, V, As, Co, Mn, Na and Si in **Fig. S1 A-H** of the Supplement. The Mann-Witney *U* test for the difference in element concentration between four physio-geographical zones demonstrated significant (at $p < 0.05$) differences for the 0.22 μm and 3 kDa fractions (**Table S3 A and B**, respectively), but not for the <50 kDa fraction (not shown). It can be seen from this table that, for both <0.22 μm filtrates and < 3 kDa ultrafiltrates, the differences between zones were pronounced for a limited number of elements in the southern part of the WSL (between forest-steppe and southern taiga); these differences were significant for a large number of elements in the northern part of the transect between middle taiga and northern taiga.

The U test for the difference in element concentration in 0.22 μm, 50 kDa and 3 kDa filtrate and ultrafiltrate for the full dataset demonstrated significant ($p < 0.05$) differences in SO_4, Si, V, Fe, Cu, As, Y, Zr, Sb, Cs, REE, Pb and U concentration in the 0.22 μm and the 3 kDa fractions and in Cl, SO_4, Si, P, K, V, Fe, Ni, As, Sr, Y, Zr, Sb, Cs, Ba, REE, Pb and U concentration in the 50 kDa and the 3 kDa fraction, but with limited difference in element concentrations between the 50 kDa and the 0.22 μm fractions (**Table S4** of the Supplement).

The average fraction of total colloids (3 kDa - 0.22 μm) in the WSL amounted to 20–80% for a number of major and trace elements (Fig. 4). Based on this histogram, we tentatively distinguished two main group of elements depending on the share of colloids: (1) Cl, Na, P, K, Si, Mg, Ca, Sr, Ba, Al, Cr, Mn, Co, Ni, Zn, Mo, Rb and Cd that exhibited between 10 and 30% of colloidal fraction and (2) SO_4, Fe, V, As, V, Cs, Sb, Y, REE, Zr, Pb and U whose colloidal fraction ranged between 30 and 80%.

3.2. Potential colloidal carriers

Based on general knowledge of major colloidal carriers of trace elements in surface waters of the WSL (Shirokova et al., 2013; Pokrovsky et al., 2016a, 2016b; Krickov et al., 2019), we tested the impact of DOC, Fe and Al concentration (in the <0.22 μm fraction) on elemental concentration in the colloidal (3 kDa–0.22 μm) forms (Table 2). The Spearman rank order correlations demonstrated significant ($p < 0.05$) impact of $DOC_{<\ 0.22\ \mu m}$ concentration on the colloidal forms of Na, Mg, Si, Ca, Sr, Zr, Ba and $Al_{<\ 0.22\ \mu m}$ concentration and on colloidal forms of Na, Mg, Si, Ca, Sr, Zr and Cs. Presumably, DOC and Al are important colloidal carriers in melted snow and they approximate aerosol organic constituent matter and the fine fraction of clays, respectively. Note that $[Al_{<0.22\ \mu m}]$ exhibited the highest correlation with colloidal Si (R_S = 0.54, $p < 0.05$; Table 2). In contrast, iron, which often acts as a main colloidal consituent in the WSL surface waters (i.e., Pokrovsky et al., 2016a, 2016b), exhibited sizable correlations only with Na, Ca, Zn, Rb, Zr and Ba, and these correlations were generally lower (except Zn, Rb, and Ba) than those with other major colloidal constituents. Given that a

Table 1
Mean values with s.d. (median with IQR in parentheses) of dissolved (< 0.22 μm), colloidal (< 50 kDa) and low molecular weight ($LMW_{<3\ kDa}$) forms of elements in snow water across western Siberia Lowland. For individual colloidal fractions measured in each natural zone of the WSL, please refer to Fig. 3 and Table S1.

Component, unit	< 3 kDa	< 50 kDa	< 0.22 μm
DOC, mg/l	0.10 ± 0.10* (0.10 ± 0.10)*	0.10 ± 0.10* (0.10 ± 0.10)*	0.81 ± 0.11 (0.81 ± 0.14)
Cl, mg/l	0.15 ± 0.18 (0.089 ± 0.11)	0.23 ± 0.15 (0.22 ± 0.17)	0.18 ± 0.21 (0.11 ± 0.12)
SO_4, mg/l	0.14 ± 0.083 (0.11 ± 0.06)	0.5 ± 0.2 (0.46 ± 0.24)	0.49 ± 0.22 (0.43 ± 0.25)
B, μg L^{-1}	0.48 ± 0.29 (0.39 ± 0.26)	0.4 ± 0.22 (0.44 ± 0.29)	0.61 ± 0.49 (0.45 ± 0.44)
Na, μg L^{-1}	77 ± 115 (39 ± 49)	59 ± 73 (34 ± 29)	85 ± 129 (42 ± 64)
Mg, μg L^{-1}	15 ± 15 (11 ± 12)	15 ± 10 (12 ± 12)	20 ± 19 (15 ± 16)
Al, μg L^{-1}	4.6 ± 5.7 (3 ± 2.6)	5.3 ± 5.8 (3.6 ± 3)	5 ± 5.3 (3.2 ± 2.3)
Si, μg L^{-1}	12 ± 5.6 (11 ± 5.9)	14 ± 3.6 (15 ± 3.6)	16 ± 4.3 (16 ± 5.5)
P, μg L^{-1}	5.2 ± 3.6 (3.9 ± 2.6)	11 ± 8.5 (9.4 ± 7.8)	5.7 ± 6.1 (3.8 ± 4.4)
K, μg L^{-1}	31 ± 20 (26 ± 20)	36 ± 43 (21 ± 7.3)	31 ± 24 (23 ± 17)
Ca, μg L^{-1}	170 ± 449 (72 ± 107)	122 ± 105 (72 ± 119)	120 ± 106 (82 ± 128)
V, μg L^{-1}	0.057 ± 0.039 (0.047 ± 0.034)	0.077 ± 0.041 (0.071 ± 0.035)	0.082 ± 0.046 (0.076 ± 0.05)
Cr, μg L^{-1}	0.057 ± 0.029 (0.047 ± 0.031)	0.06 ± 0.03 (0.049 ± 0.035)	0.068 ± 0.032 (0.06 ± 0.031)
Mn, μg L^{-1}	1.4 ± 1.2 (1.1 ± 1.5)	1.8 ± 2.2 (0.91 ± 1.4)	1.7 ± 1.5 (1.3 ± 1.5)
Fe, μg L^{-1}	1.9 ± 2 (1.1 ± 1.5)	2.5 ± 2.4 (2.1 ± 1.2)	2.9 ± 2.4 (2.2 ± 1.8)
Co, μg L^{-1}	0.011 ± 0.011 (0.0074 ± 0.0086)	0.017 ± 0.022 (0.011 ± 0.0074)	0.013 ± 0.014 (0.009 ± 0.011)
Ni, μg L^{-1}	0.059 ± 0.026 (0.053 ± 0.032)	0.076 ± 0.047 (0.049 ± 0.081)	0.057 ± 0.036 (0.045 ± 0.039)
Cu, μg L^{-1}	0.17 ± 0.11 (0.17 ± 0.13)	0.16 ± 0.078 (0.14 ± 0.052)	0.24 ± 0.17 (0.22 ± 0.16)
Zn, μg L^{-1}	7.6 ± 12 (3.6 ± 3.5)	11 ± 25 (3.2 ± 1.8)	8.3 ± 14 (3.4 ± 3.9)
Ga, μg L^{-1}	0.0017 ± 0.0017 (0.0011 ± 0.0016)	0.0019 ± 0.0022 (0.0011 ± 0.0013)	0.0019 ± 0.002 (0.0012 ± 0.0015)
As, μg L^{-1}	0.21 ± 0.14 (0.17 ± 0.12)	0.29 ± 0.15 (0.24 ± 0.089)	0.32 ± 0.19 (0.26 ± 0.12)
Rb, μg L^{-1}	0.037 ± 0.026 (0.029 ± 0.027)	0.041 ± 0.036 (0.033 ± 0.028)	0.043 ± 0.032 (0.036 ± 0.035)
Sr, μg L^{-1}	0.51 ± 0.68 (0.23 ± 0.35)	0.99 ± 1.2 (0.41 ± 0.72)	0.81 ± 1.23 (0.3 ± 0.56)
Y, μg L^{-1}	0.0027 ± 0.007 (0.00082 ± 0.001)	0.0041 ± 0.0065 (0.0027 ± 0.0021)	0.0053 ± 0.0077 (0.0032 ± 0.0024)
Zr, μg L^{-1}	0.001 ± 0.00073 (0.00067 ± 0.001)	0.002 ± 0.0014 (0.0011 ± 0.0024)	0.0025 ± 0.002 (0.0018 ± 0.0021)
Mo, μg L^{-1}	0.010 ± 0.008 (0.0075 ± 0.0087)	0.012 ± 0.01 (0.0078 ± 0.0056)	0.013 ± 0.011 (0.01 ± 0.0076)
Cd, μg L^{-1}	0.025 ± 0.011 (0.025 ± 0.016)	0.029 ± 0.011 (0.033 ± 0.017)	0.03 ± 0.012 (0.028 ± 0.019)
Sb, μg L^{-1}	0.017 ± 0.031 (0.0085 ± 0.0085)	0.022 ± 0.012 (0.016 ± 0.012)	0.029 ± 0.039 (0.017 ± 0.014)
Cs, μg L^{-1}	0.0012 ± 0.0008 (0.001 ± 0.00076)	0.0017 ± 0.001 (0.0014 ± 0.0009)	0.0018 ± 0.001 (0.0017 ± 0.0012)
Ba, μg L^{-1}	0.56 ± 0.63 (0.31 ± 0.47)	1.1 ± 1.0 (0.64 ± 1.4)	0.75 ± 0.81 (0.43 ± 0.81)
La, μg L^{-1}	0.0029 ± 0.0095 (0.00055 ± 0.0011)	0.0045 ± 0.0067 (0.0024 ± 0.0019)	0.004 ± 0.0052 (0.0027 ± 0.0021)
Ce, μg L^{-1}	0.0037 ± 0.010 (0.00079 ± 0.0016)	0.0084 ± 0.012 (0.0048 ± 0.004)	0.0082 ± 0.01 (0.0055 ± 0.004)
Yb, μg L^{-1}	0.00019 ± 0.00046 (0.00007 ± 0.000061)	0.00035 ± 0.00053 (0.00022 ± 0.00016)	0.00038 ± 0.00057 (0.00025 ± 0.00016)
Pb, μg L^{-1}	0.43 ± 0.25 (0.37 ± 0.23)	0.58 ± 0.25 (0.61 ± 0.27)	0.67 ± 0.31 (0.63 ± 0.28)
U, μg L^{-1}	0.00071 ± 0.0012 (0.00034 ± 0.00030)	0.00083 ± 0.001 (0.00054 ± 0.00049)	0.0009 ± 0.0011 (0.00054 ± 0.00053)

* maximal concentration, corresponding to the quantification limit by Shimadzy instrument. In case if the s.d. of mean (or IQR of median) for a given element exceeds the difference between the values in different fractions, this means non- measurable amount of this element in the 3 kDa–50 kDa fraction or the 50 kDa – 0.22 μm fraction.

sizable proportion of sulfate resided in the colloidal fraction (Fig. 4), sulfate in the snow water was also tested as a potential colloidal carrier of other major and trace elements. We found that the concentration of SO_4 exhibited significant ($p < 0.05$) correlations with the largest number of colloidal elements (Na, Si, Ca, Zn, Sr, Zr, Cs and Ba). Note that the pH of the snow water did not exhibit any sizable ($p < 0.05$) correlation to the colloidal proportion of major and trace elements (Table 2).

The latitudinal pattern of colloid stoichiometry exhibited either a northward increase in Organic Carbon (OC): element mole ratio (i.e., OC: Ca, OC: SO_4, OC: Fe and SO_4: Ca) or a local depletion in Al relative to Fe, SO_4 and Ca in the southern taiga zone (**Fig. S2**). The OC: Al, SO_4: Fe and Ca: Fe ratios in the colloids did not vary across the south-north transect (**Fig. S2**). When averaged over the entire area of western Siberia, the molar OC: SO_4: Ca: Al: Fe stoichiometry of major colloidal (3 kDa–0.22 μm) carriers ranged from 2000:175:39:1.4:1 in the south of the WSL to 3000:180:37:1.6:1 in the north (**Table S5** of the Supplement).

3.3. Impact of pollution point source on element concentrations and proportions of colloids

To better constrain the sources of elements in the snow water, we attempted distinguishing between local and global (far range) transfer. For this, we defined the distance to the nearest human-related object (gas flare, small settlement located within the initial 20 km of a sampling point, or large town) taking into account the dominant wind direction during winter as detailed in **Table S6** of the Supplement. The components of the total dissolved fraction (<0.22 μm) of snow water that were impacted by distance to potential contamination objects were major anions and cations, alkaline-earth and divalent transiotion metals, toxic metals (Zn, Cd), some geochemical tracers (Al, Ga, Y, Zr, REE, U) and Mo as illustrated in Fig. 5 **A-F** and **Table S2 A**. For the $LMW_{<3\ kDa}$ fraction, only alkaline-earth metals, Rb, Al, Fe, Ga, V, Mn, Cd and U demonstrated significant ($p < 0.01$) correlations with the distance to the local pollution center (**Table S2 B**). We thus suggest that, in addition to far-range atmospheric transfer, these elements are strongly controlled by multiple sources of local (< 20 km) and near-local (20–100 km) pollution.

We also tested the link between the proportion of colloidal forms of elements in snow and the distance to the local pollution spot. The majority of solutes affected by the point sources (SO_4, K, Ca, Cr, V, Fe, Co, Ni and Cd) did not exhibit any link ($R^2 < 0.2$; $p > 0.05$) between their colloidal fraction and distance. Only for P, Mn, Zn and Ba were the colloidal forms significantly ($R^2 > 0.2$; $p < 0.05$) affected by the distance to a potential contamination spot (Fig. 6 **A-D**).

4. Discussion

4.1. Snowmelt is capable of providing a sizeable amount of trace elements in riverine flux during spring flooding in western Siberia

The unprecedented geographical coverage and assessment of the full depth of the snow cover performed in the present study allowed for quantification of snowmelt impact on riverine fluxes of major and trace elements in western Siberia at the scale of whole watersheds. The ratio of the winter-period stock of the dissolved (< 0.22 μm) fraction of snow to the mean dissolved spring-time flux of small and medium-size rivers across all latitudinal zones of the WSL is illustrated in Fig. 7. For simplicity, we considered average concentration of trace elements in snow water from two zones of the territory: the southern (54.5–60°N) and the northern (60–66.5°N) parts of the WSL as detailed in **Fig. S3.** For

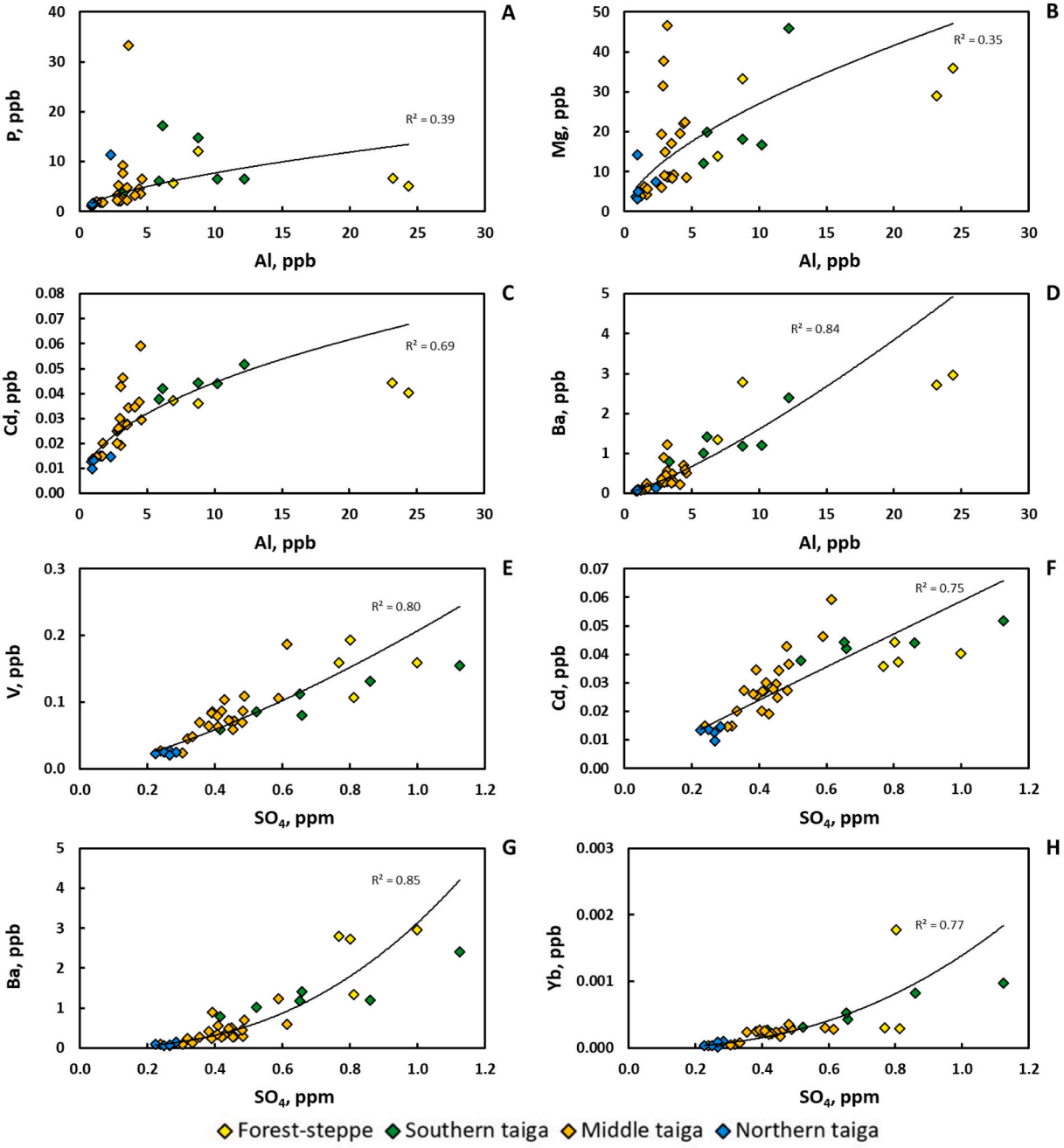

Fig. 2. Pairwise correlations between elements in the 0.22 μm fraction of snow water illustrating the impact of Al on P, Mg, Cd and Ba (A-D) as well as SO_4 on V, Cd, Ba and Yb (*E*-H).

this calculation, we used the snow volume (in millimeters of water) accumulated over a full winter which is fairly well known for Western Siberia (Karnatzevicth and Khruschev, 2014; Shevchenko et al., 2017) and ranges from 110 to 120 mm in the 56–60°N zone to 140–150 mm in the northern part of the Ob River basin (60–68°N). The spring-time river runoff (in mm during May and June) was taken as calculated in Pokrovsky et al. (2020).

These first-order mass balance calculations demonstrate that in the southern, permafrost-free zone, more than half of spring-time riverine export of the total dissolved fraction (< 0.22 μm) Cd, Zn, Pb, Cs and Sb can be provided by snowmelt (**Fig. S3 A**). In the northern, permafrost-affected part of the WSL, riverine export of the <0.22 μm fractions of Pb, Cd, Zn, As, Sb, Cs, SO_4 and Cu during spring flooding can be sizably (> 30%) impacted by snowmelt (**Fig. S3 C**). The elements mostly affected by snowmelt are Cd, Pb and Zn whose riverine fluxes are 2–4 times lower than the input from the snowpack (Fig. 7 **A**). Given the excess of these metals in the snowpack relative to the riverine export, we hypothesize that during snowmelt and surface water influx into the river a sizable share of these metals, which are present in the snowpack, may be retained by ground vegetation, scavenged in river and lake sediments or adsorbed onto river suspended matter (> 0.22 μm) and thereby transported in particulate form from land to ocean.

The effect of the snow water on the low molecular weight (truly dissolved and potentially bioavailable fraction) in the river flux is more drastic. The $LMW_{< 3\ kDa}$ riverine fluxes of Pb, Cd, Zn, Cr, Cs, Ce, Ga, Sb, Y, Co, heavy REEs and Cu in the south and Pb, Cd, Zn, Cu and As in the north are strongly (≥ 50%) affected by the snowmelt (**Fig. S3 B**). A mass-balance comparison of the $LMW_{< 3\ kDa}$ stocks in snow and the spring-time $LMW_{< 3\ kDa}$ export fluxes (Fig. 7 **B** and **Table S7** of the Supplement) demonstrates that the majority of riverine fluxes of Zn, Cd, As, Pb,

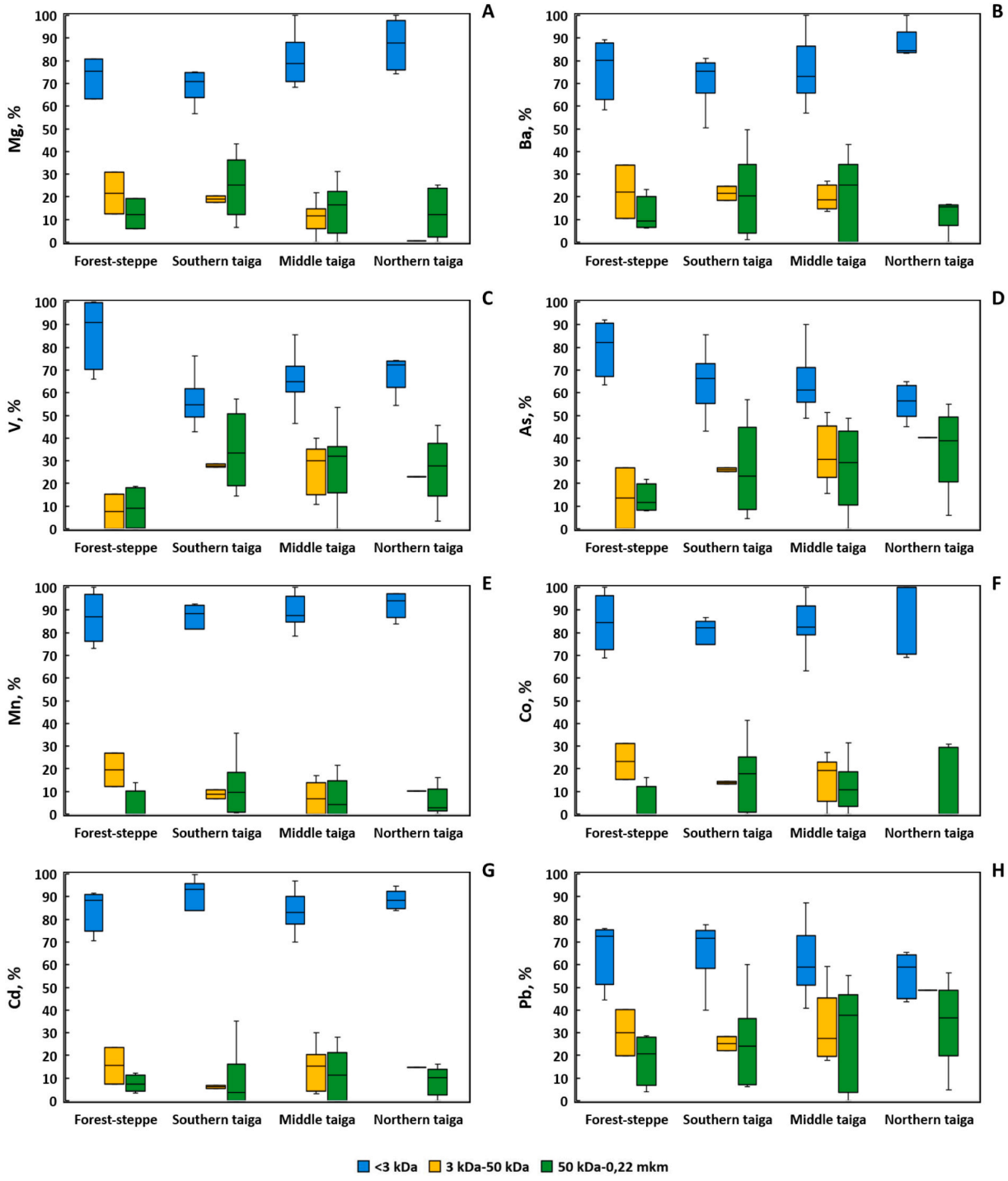

Fig. 3. Median (with IQR) values of colloidal (medium molecular weight, $MMW_{3–50\ kDa}$ and high molecular weight, $HMW_{50\ kDa\ -\ 0.22\ \mu m}$) and low molecular weight ($LMW_{<\ 3\ kDa}$) fractions in snow water averaged for each biome of the WSL.

Cu and Sb in the LMW form during spring freshet can be provided via snowmelt. However, among these elements, divalent transition metal cations, trivalent and tetravalent hydrolysates are unlikely to remain in the LMW forms in the river water. This is because, upon their release into freshet surface waters enriched in DOM, these cations transform into organic colloids (Krickov et al., 2019). In contrast, snowmelt could be responsible for delivery of almost half of the trace oxyanions (As and Sb) present in the LMW form in river waters.

Overall, these comparisons demonstrate the highly important and previously underestimated impact of snowfall on spring flood time period riverine export not just on total dissolved fraction, but also on the $LMW_{<\ 3\ kDa}$ fraction and thus potentially bioavailable trace elements in western Siberia. Given that the freshet period accounts for >40–50% of the total annual lateral export of riverine solutes (Pokrovsky et al., 2020), changes in winter-time atmospheric precipitation may play an overwhelming role in inland aquatic ecosystem response to on-going climate change. The complexity of this response is thought to be related to two main factors: quantity of the precipitation and total dissolved chemical composition of snow water. The present study confirms the importance of snow water solutes in riverine export but also adds another dimension that was previously unknown: colloidal and low molecular weight inorganic solutes of the snowpack. Particular feature

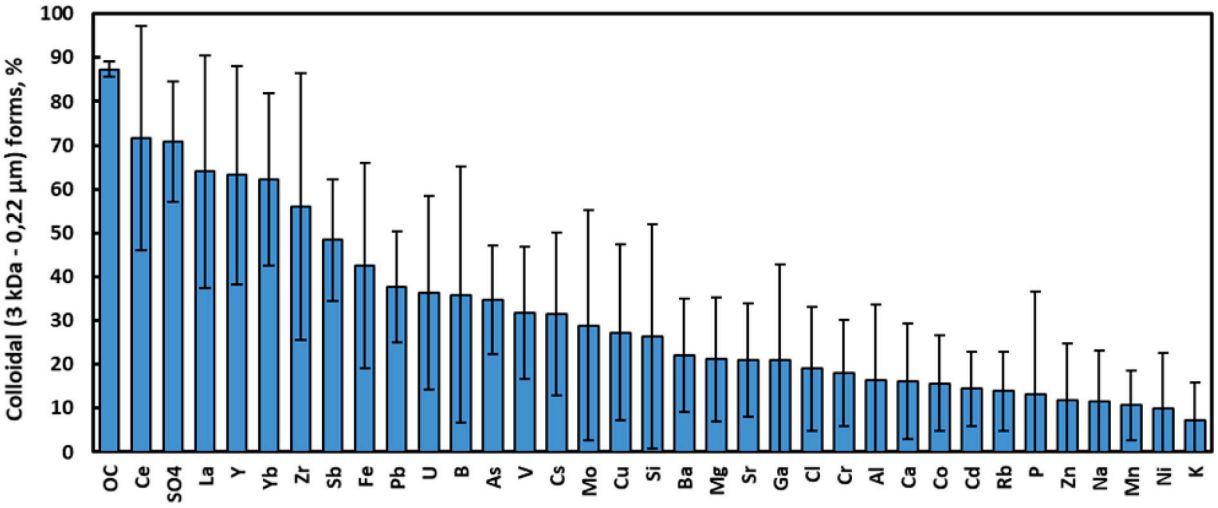

Fig. 4. Average (with s.d.) colloidal (3 kDa – 0.22 µm) fractions in snow water across all WSL zones. Percentage for DOC is calculated assuming a quantification limit in the 3 kDa fraction (0.1 ± 0.1 mg L^{-1}). This value is likely to be underestimated.

Table 2
Spearman Rank Order Correlations between the percentage of colloidal forms (3 kDa - 0.22 µm) of major and trace elements and the concentration of main potential colloidal carriers (DOC, SO_4, Al and Fe in the 0.22 µm filtrate). Marked correlations (*) are significant at $p < 0.05$.

Colloids	pH	Ca (0.22 µm)	DOC (0.22 µm)	SO_4 (0.22 µm)	Al (0.22 µm)	Fe (0.22 µm)
Cl	0.12	−0.34*	−0.22	−0.43*	−0.43*	−0.44*
SO_4	−0.24	−0.20	0.08	−0.06	−0.13	0.02
B	−0.02	0.01	0.08	−0.25	−0.23	−0.19
Na	0.02	0.72*	0.63*	0.50*	0.68*	0.38*
Mg	0.06	0.52*	0.36*	0.34	0.50*	0.21
Al	0.28	−0.17	−0.25	−0.15	−0.24	−0.38*
Si	−0.10	0.49*	0.42*	0.46*	0.54*	0.27
P	−0.29	0.32	0.31	0.22	0.32	0.15
K	0.33	0.21	0.11	0.01	0.17	−0.05
Ca	0.28	0.57*	0.37*	0.35*	0.37*	0.37*
V	−0.25	0.13	0.31	−0.01	0.01	−0.12
Cr	−0.16	0.26	0.25	0.15	0.18	−0.06
Mn	0.10	0.22	0.23	0.19	0.16	0.19
Fe	0.06	0.09	0.08	0.07	−0.05	−0.11
Co	0.18	−0.01	−0.02	−0.07	−0.07	−0.11
Ni	0.28	0.29	−0.01	0.25	0.12	0.33
Cu	0.25	0.25	0.28	0.19	0.30	0.11
Zn	0.08	0.40*	0.29	0.41*	0.29	0.48*
Ga	0.19	0.36*	−0.17	0.21	0.17	0.03
As	−0.22	−0.29	0.11	−0.38*	−0.29	−0.32
Rb	0.13	0.30	0.14	0.32	0.16	0.37*
Sr	−0.03	0.54*	0.68*	0.36*	0.51*	0.22
Y	−0.09	0.11	0.13	0.06	−0.03	−0.09
Zr	−0.23	0.54*	0.60*	0.66*	0.60*	0.49*
Mo	0.28	0.34	0.32	−0.03	0.22	−0.17
Cd	0.10	0.12	0.17	0.01	−0.02	0.07
Sb	−0.14	−0.44*	0.00	−0.39*	−0.35*	−0.27
Cs	0.00	0.31	0.32	0.35*	0.39*	0.25
Ba	−0.05	0.38*	0.37*	0.42*	0.31	0.43*
La	0.21	0.11	0.20	0.04	−0.03	−0.16
Ce	0.10	0.15	0.31	0.05	−0.01	−0.17
Yb	0.15	0.24	0.33	0.14	0.14	0.05
Pb	0.08	0.02	0.06	−0.12	−0.16	−0.07
U	0.22	0.07	0.04	0.01	−0.03	−0.21

of snow water colloids is that they have sizable proportion of inorganic constituents, such as Ca and SO_4, in contrast to surface water colloids which are dominated by organic associations.

4.2. *Impact of local pollution versus global atmospheric transfer on the total dissolved and low molecular weight fraction of western Siberian snow*

The impact of pollution sources on major and trace element concentrations established in the WSL is consistent with former studies of local pollution impact on the chemical composition of snow. Generally, a distance of 10 to 20 km is reported as the range where impact of a local pollution source is most pronounced (Jaffe et al., 1995; Walker et al., 2003; Javed et al., 2022). Thus, Walker et al. (2003) analyzed snow water in the European Arctic and demonstrated elevated concentrations of elements associated with alkaline combustion ash around the coal mining towns of Vorkuta and Inta. The increases in concentrations of Ca, K, Sr, Mn, Ba, Sr and As were pronounced within a distance of 10 to 20 km around the local point source of pollution. Other studies of point pollution impact on snowpack chemical composition demonstrated significant increase in dissolved concentrations of Cu, Ni, Co and As in the vicinity of the nickel industry (Reimann et al., 1996). The latter authors distinguished four different sources of these elements in the snow pack whose role varied depending on proximity to a local pollution source: industrial emissions, sea spray, geogenic dust and anthropogenic dust. Telmer et al. (2004) demonstrated that dissolved Cu, Pb, and Zn have a strong enrichment near the metal smelter (Quebec) and exhibit strong negative correlation with distance (up to 45 km), indicating that the smelter is the dominant source of such elements to regional snowpack. At the same time, Mn, K, Rb and Cs had little to no relationship to the smelter and any emission of these elements by the smelter was suggested to be minimal compared to long-range delivery from natural emissions.

The total and dissolved concentrations of 29 metals and metalloids were analyzed in the snowpack collected in the Athabasca oil sand region of Canada (Guéguen et al., 2016) and based on the depositional pattern in this industrial region three groups of elements were found: 1) V and Mo showing significant exponential decrease with distance, suggesting oil sands development sources; 2) Al, Sb, As, Ba, Fe, Ni, Tl, and Ti and Zn exhibiting exponential decline patterns but with some local point sources, and 3) Cd, Cl, Cr, Mn, Sr and Th whose depositional pattern represents local sources. The background sites located at a distance of 25–35 km from Tyumen City were characterized by increased concentrations of dissolved Cd, Cu, Zn, Pb, Ni, As and Mo when compared to average levels documented in the snowpack of Western Siberia (Moskovchenko et al., 2021). A similar assemblage of pollutants is also reported from metallurgical districts of the Southern Ural (Udachin, 2012) which are located 250–350 km southwest of Tyumen. Due to the predominance of the southern and southwestern winds in the study area

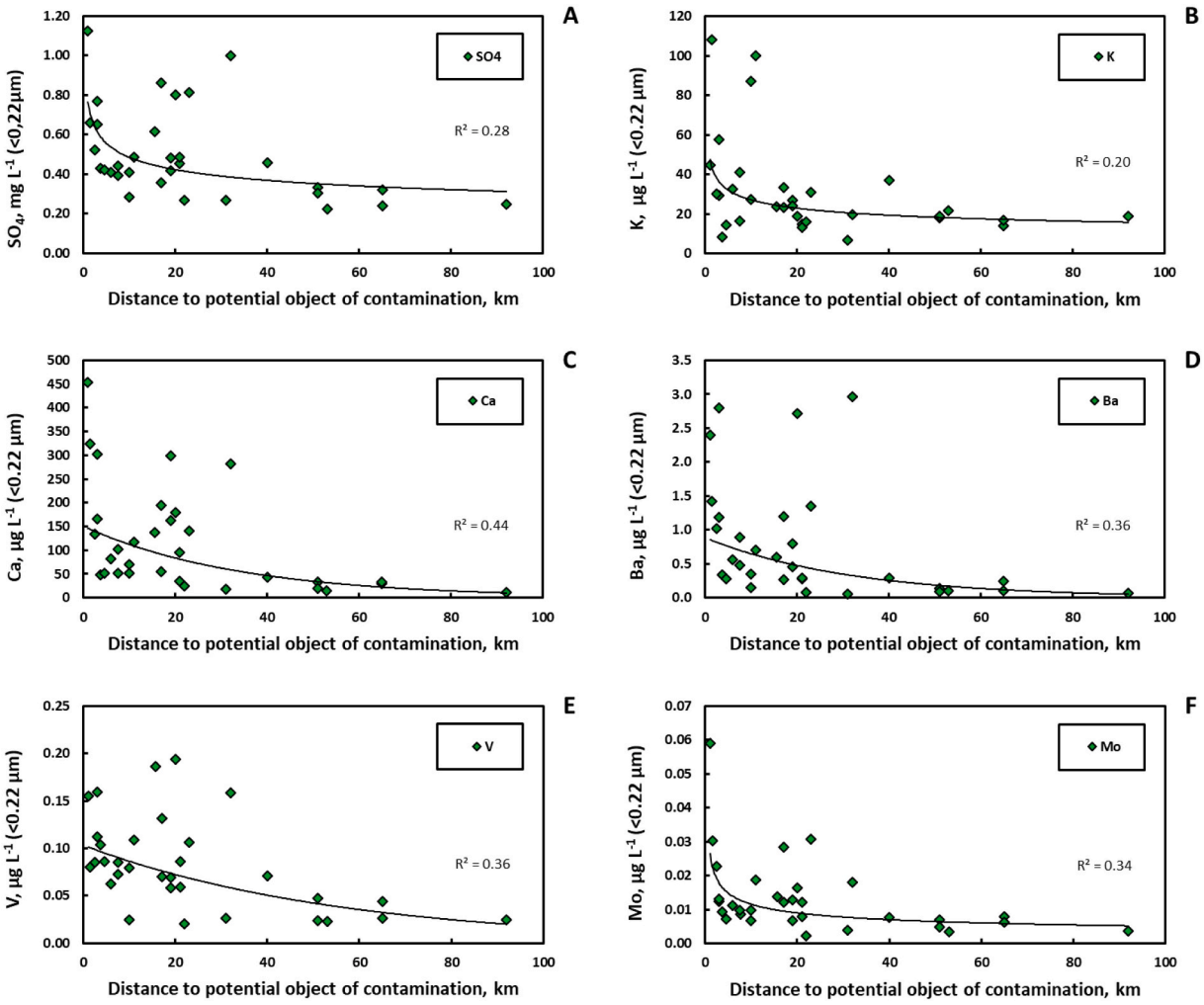

Fig. 5. Examples of dissolved (<0.22 µm) metal concentrations in snow water as a function of.
distance to potential objects of contamination in the WSL. A full list of elements exhibiting significant ($p < 0.01$) impact from local pollution centers for the <0.22 µm and < 3 kDa fractions is provided in **Table S2**.

during winter, increased concentrations of these elements can be explained via long-range atmospheric transport from the Urals (Moskovchenko et al., 2021).

Overall, the results of the present study are consistent with previous works on the importance of local pollution spots in the formation of total dissolved (< 0.22 or 0.45 µm) load of the snow water. The elements indicative for pollution sources in the WSL are quite diverse, ranging from major cations and anions (SO_4, K, Ca) to alkaline-earth metals and heavy metal pollutants. At the same time, this study adds a new previously unknown feature to pollution impact in demonstrating an increase in the colloidal (3 kDa - 0.22 µm) forms of several environmentally important elements such as P, Mn, Zn and Ba in the vicinity of local pollution sources.

4.3. Snow water colloids are rich in SO_4 and Ca and present a sizable contrast with humic surface waters

The colloids of the snow water characterized in this study are drastically different from colloids identified in earlier works on surface waters of western Siberia. Unlike humic freshwater colloids, these meltwater colloids are rich in Ca and SO_4 and poor in Fe and Al and cannot be qualified as purely organo-iron / organo-aluminium entities. Indeed, the average colloidal stoichiometry of the WSL snow water ($(OC)_{2890}(SO_4)_{180}Ca_{37}Al_{1.56}Fe_1$) is sizably different from that of soil porewaters ($OC_{200\text{-}600}Fe_{0.5\text{–}1.5}Al_{1.0}$) as documented by Raudina et al. (2021) and Lim et al. (2022), river waters ($OC_{260\text{-}860}Ca_{2\text{-}3}Fe_{1\text{-}7}Al_{1.0}$) as documented by Krickov et al. (2019), and peat ice ($OC_{500\text{-}2000}Fe_{1\text{–}1.5}Al_{1.0}$), as documented by Lim et al. (2022).

The exact mechanisms of colloid generation in atmospheric aerosols remain poorly understood but may include the disintegration of flying ash particles, condensation of volatile forms of industrial fumes, or dissolution/dispersion of soil minerals such as clays. It should also be noted that an extremely low ionic strength of meltwater (S.C. = 10 ± 2 µS cm^{-1}) facilitates clay dispersion, leading to generation of colloidal particles with large diffusional layer (Russel et al., 1989). The low salt concentration also enhances the stability of colloidal particles given that the increasing electrolyte concentration inhibits colloidal dispersion and facilitates flocculation (van Olphen, 1977). Therefore, a combination of specific sources contributing to the origin of dissolved elements in the snow and specific processes operating within atmospheric aerosols during winter period may shape the chemical composition of snow water colloids as discussed below.

The freezing of solutes in the sea and on the land may enrich atmospheric aerosols in salts. Clusters of these sparingly soluble compounds (i.e., $CaSO_4$, $CaCO_3$), having sizes <0.22 µm but larger than simple ions or molecular complexes, can temporary persist after thawing of snow, despite solution being undersaturated with respect to relevant solid phases. A likely source of major sea salt in snow aerosols is frost flowers that are formed on Arctic sea ice (i.e., Barber et al., 2014; Rankin et al., 2000; Alvarez-Aviles et al., 2008; Lim et al., 2019). The colloidal

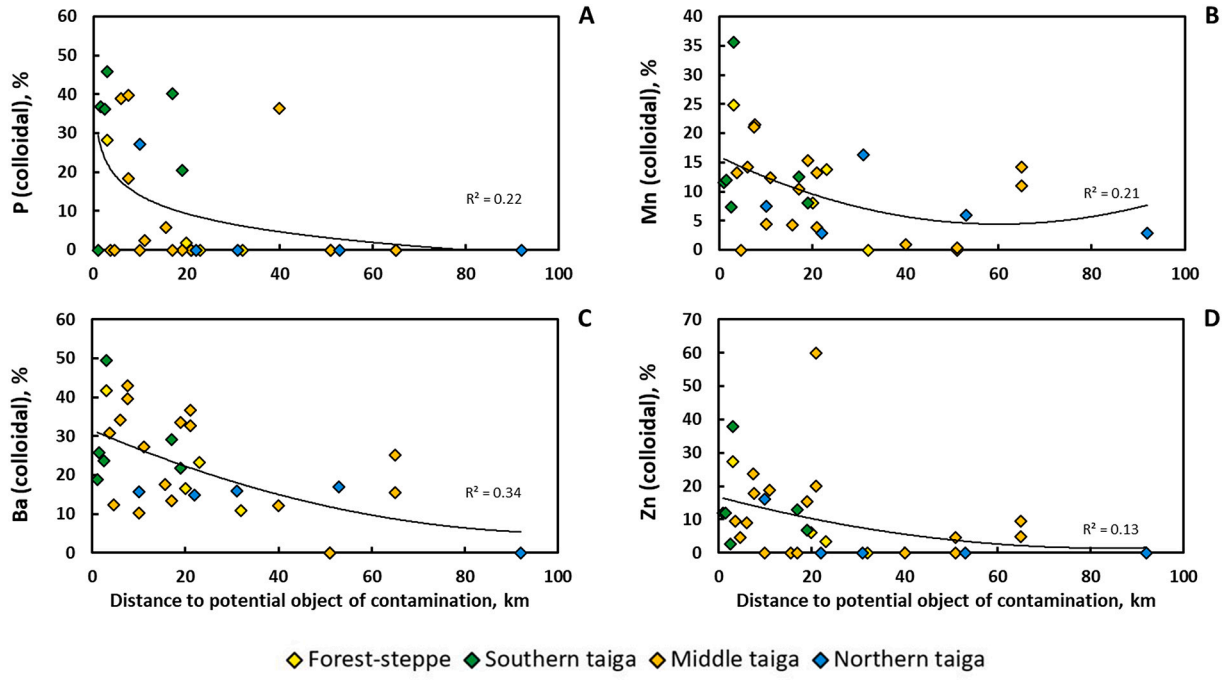

Fig. 6. Decrease in proportion of colloidal (3 kDa - 0.22 μm) forms of P_{tot} (**A**), Mn (**B**), Ba (**C**) and Zn (**D**) with distance to potential contamination objects.

composition of these presumably soluble (< 0.22 μm) aerosols is not known but it is not excluded that some fraction of these salts is present in the ionic associates or ikaite ($CaCO_3 \times 6H_2O$) particles (Rysgaard et al., 2013) larger than 3 kDa. Hydrated calcium carbonate is capable of retaining some divalent alkaline-earth metals similar to calcite and aragonite. Divalent cations coprecipitation with Ca sulfate is also possible (Deng et al., 2013; Ma et al., 2020). Altogether, this can explain the co-existence of a sizable proportion of alkaline-earth metals in the colloidal fraction of the snow water, given that Ca concentration in the <0.22 μm fraction is an order of magnitude higher than that of Mg and Zn and two orders of magnitude higher than that of other alkaline-earth metals.

In a similar way, thermokarst lakes which freeze solid may contribute to generation of organo-ferric colloids. In the WSL, the freezing of abundant thermokarst lakes leads to complete ice formation with seeps of deep, organic and Fe-rich waters on the surface that are detectable in the end of winter (Manasypov et al., 2015). Such seeps may generate some colloidal particles after freezing of this water, similar to the frost flowers generated from the Arctic ice. Sulphur dioxide emissions and associated trace metal pollutants are frequently detected in the dissolved and particulate load of the snow water (i.e., Walker et al., 2003).

Both methanesulphonic acid and non-sea salt sulfate can contribute to the SO_4 concentration in atmospheric aerosols (Jung et al., 2020). Further, gaseous adsorption of SO_2 on the snow surface (Thakur and Thamban, 2019) followed by S(IV) → S(VI) oxidation can also contribute to the ionic and colloidal load of sulphate in the snow water. Under these conditions, mobilization of other soluble oxyanions (B, As, Mo and Sb) together with subcolloidal SO_4 forms in the snow water may become possible. Note that, in the atmospheric aerosols, the oxyanions are known to form double (S, Se) or triple (N, P, As) bonds with carbon (Goldstein and Galbally, 2007).

Organic aerosols are present in both micro- and nano-particulate form and can exist in different phases including liquid, semi-solid and solid, or glassy depending on temperature and relative humidity (Knopf et al., 2018). As a result, organic matter (OM) present in snow water colloids is likely to include (*i*) organic aerosols such as stearic and cis-pinonic acid (Luo and Yu, 2010), (*ii*) humic-like compounds (Graber and Rudich, 2006), (*iii*) black carbon in the form of sooty subcolloidal particles (Nichman et al., 2019), (*iv*) OM-coated mineral dust (such as feldspar or kaolinite, Knopf et al., 2018). Although studying the exact molecular nature of DOM in the colloidal and LMW fractions of snow water was beyond the scope of this sudy, relatively high ratios of carbon to SO_4 and cations in the colloids (**Fig. S2**) suggest a dominance of organic aerosols, black carbon and humic-like compounds in snow water rather than organo-iron and organo-alluminium associates typical of inland waters in permafrost peatlands.

The nature of colloidal trace metals in snow waters also remains poorly constrained. Miler and Gosar (2015) demonstrated that anthropogenic metal-bearing phases in snow particles are represented by irregular ferrous oxides, ferrous alloys, spherical ferrous oxides, and ferrous silicates with variable contents of Cr, Mn, Ni, V, W and Mo. They also identified secondary weathering products such as Al silicates, Fe oxy-hydroxides and Fe oxy-hydroxy sulfates with minor contents of transition metals. It can be hypothesized that some solid aerosol particles can de disintegrated to fine fractions (< 0.22 μm) and partially contribute to the colloidal load of snow waters. Low solubility-low mobility elements that are present in a sizable amount of the colloidal fraction in river, lake and soil waters of western Siberia with Fe, Al hydroxides and organic matter as main colloidal carriers (Pokrovsky et al., 2016a, 2016b; Krickov et al., 2019; Raudina et al., 2021) are much less abundant in snow water from this region. In fact, concentrations in the <0.22 μm fraction of the snow water of DOC (0.6 to 1.0 mg L^{-1}), Fe (1 to 10 μg L^{-1}) and Al (1 to 15 μg L^{-1}) are quite low for accommodating a sizable proportion of other trace metals. Consistent with this, correlations of these elements with the colloidal fraction of other trace elements were quite low whereas the concentraton of SO_4 and Ca exhibited significant ($p < 0.05$) correlations with the colloidal fraction of the largest number of elements (Na, Si, Zn, Sr, Zr, Cs and Ba). It is thus not excluded that Ca- and SO_4-rich colloids in the meltwater also accommodate some trace metals.

An additional factor of colloid generation and transformation in the aerosols is freeze-thaw cycles (FTC), which may become especially pronounced at the beginning and end of the winter season. Colloidal load of boreal and subarctic freshwaters is subjected to strong modification under freeze-thaw regimes; these cycles can produce large

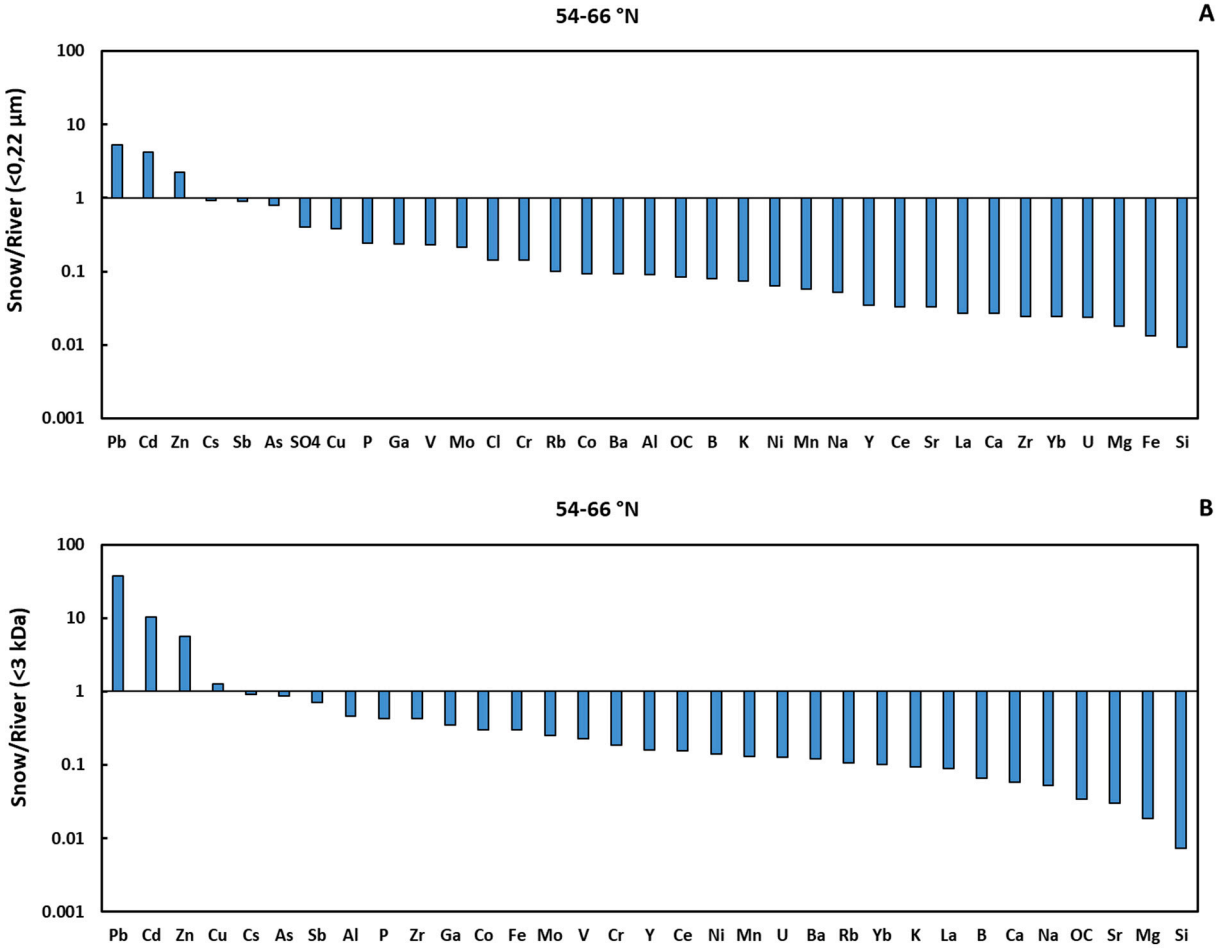

Fig. 7. The ratio of winter-period stock of dissolved$_{< 0.22\ \mu m}$ (**A**) and LMW$_{< 3\ kDa}$ (**B**) fractions of snow water (from this study) to the mean dissolved spring-time flux for small and medium-size rivers averaged across across all latitudinal zones of the WSL (54–66°N). For this calculation, snow volume (in millimeters of water) accumulated over full winter (110–120 mm in the south and 150–150 mm in the north) and mean river runoff over May and June together with riverine concentrations (Pokrovsky et al., 2020) were used.

subcolloidal particles and generate low molecular weight organic compounds (i.e. Pokrovsky et al., 2018; Payandi-Rolland et al., 2021). However, special FTC experiments are needed to assess the degree to which these processes can impact the snow / rain water organic- sulfate- and Ca-rich colloids.

5. Conclusions

To better understand the dissolved load of major and trace elements in the snow water of western Siberia, we sampled snow cores integrated over the entire depth (0 to 50 cm) along a 2800 km south-north gradient and analyzed the concentration of solutes in the total dissolved (< 0.22 µm) colloidal (0.22 µm - 50 kDa and 50 kDa - 3 kDa) and low molecular weight (< 3 kDa) fractions. A number of major and trace metals in the snow water collected across western Siberia demonstrate a non-negligible proportion (30 to 50%) of total colloidal (3 kDa - 0.22 µm) forms. Snowfall may represent a sizable contribution of trace elements, in both total dissolved$_{< 0.22\ \mu m}$ (Cd, Pb, Zn, As, Sb and Cs) and LMW$_{< 3\ kDa}$ (Cd, Pb, Zn, As, Sb, Cs, Cu) forms, to riverine export during spring flooding in western Siberia. In addition to tracing local pollution sources by dissolved (< 0.22 µm) concentrations of SO_4, Cl, alkalis an alkaline-earths, divalent transition metals, V, Cr, Mo, Ga, Y, Zr, REE, Cd and U, we demonstrated enrichment in snow water of colloidal forms of P, Mn, Zn and Ba in the vicinity of local pollution source. The average stoichiometric composition of snow water colloids demonstrates that they are enriched in OC, Ca and SO_4 but poor in Al and Fe. In addition to anthropogenic sources of snowwater colloids (submicron particles of flying ash and other anthropogenically-derived substances), natural pathways of colloid generation may include but are not limited to: (*i*) solute freezing along thermokarst lake surfaces producing dispersed subcolloid particles (iron hydroxide and organic matter), (*ii*) frost flowers of the Arctic ice (hydrous Ca carbonate and sulfates), (*iii*) terrigenous clay dispersion/dissolution in low ionic strength snow water and (*iv*) sulphur dioxide oxidation on the snow surfaces.

Overall, we demonstratre the previously undervalued importance of colloidal forms of toxicants and geochemical tracers in the snow water. Climate warming in Siberia may not only change the quantity of snow and dissolved fraction but also the colloidal and low molecular weight forms of macro- and micronutrients and toxicants. Further quantification on the impact of atmospheric precipitation as it relates to elementary input of inland waters on an annual scale highlights the need for a systematic study of colloidal load in rain water across this territory.

Data availability

The full data set of measured DOC, major and trace element concentrations (< 0.22 µm, < 50 kDa and <3 kDa) in the snow water in all sites and different sampling depths is presented in the Mendeley portal database:

Pokrovsky, O., Krickov, I.V., Shevchenko, V., Vorobyev, S., Lim, A. (2022), "Major and trace element concentrations in the snow water of western Siberia", Mendeley Data, V1. https://data.mendeley.com/

datasets/3vnfk6s9tb.

Declaration of Competing Interest

The authors declare that they have no known competing financial interests or personal relationships that could have appeared to influence the work reported in this paper.

Data availability

https://data.mendeley.com/datasets/3vnfk6s9tb

Acknowledgements

We acknowledge support from RFBR grants No 19-05-50096, 20-05-00729, 19-29-05209 and the Tomsk State University Development Program "Priority-2030". We thank two anonymous reviewers and the Editor Don Porcelli for very insightful comments and corrections. C. Benker is thanked for editing the English of the manuscript.

Appendix A. Supplementary data

Supplementary data to this article can be found online at https://doi.org/10.1016/j.chemgeo.2022.121090.

References

Alvarez-Aviles, L., Simpson, W.R., Douglas, T.A., Sturm, M., Perovich, D., Domine, F., 2008. Frost flower chemical composition during growth and its implications for aerosol production and bromine activation. J. Geophys. Res. 113, D21304. https://doi.org/10.1029/2008JD010277.

Bagard, M.L., Chabaux, F., Pokrovsky, O.S., Viers, J., Prokushkin, A.S., Stille, P., Rihs, S., Schmitt, A.D., Dupré, B., 2011. Seasonal variability of element fluxes in two Central Siberian rivers draining high latitude permafrost dominated areas. Geochim. Cosmochim. Acta 75, 3335–3357. https://doi.org/10.1016/J.GCA.2011.03.024.

Banc, C., Gautier, M., Blanc, D., Lupsea-Toader, M., Marsac, R., Gourdon, R., 2021. Influence of pH on the release of colloidal and dissolved organic matter from vertical flow constructed wetland surface sludge deposits. Chem. Eng. J. 418, 129353 https://doi.org/10.1016/J.CEJ.2021.129353.

Barbante, C., Boutron, C., Morel, C., Ferrari, C., Jaffrezo, G.L., Cozzi, Z., Gaspari, V., Cescon, P., 2003. Seasonal variations of heavy metals in Central Greenland snow deposited from 1991 to 1995. J. Environ. Monit. 5, 328–335. https://doi.org/10.1039/b210460a.

Barber, D.G., Ehn, J.K., Pućko, M., Rysgaard, S., Deming, J.W., Bowman, J.S., Papakyriakou, T., Galley, R.J., Søgaard, D.H., 2014. Frost flowers on young Arctic Sea ice: the climatic, chemical, and microbial significance of an emerging ice type. J. Geophys. Res. Atmos. 119, 11,593–11,612. https://doi.org/10.1002/2014JD021736.

Barrie, L.A., Vet, R.J., 1984. The concentration and deposition of acidity, major ions and trace metals in the snowpack of the Eastern Canadian shield during the winter of 1980–1981. Atmos. Environ. 18 (7), 1459–1469.

Bazzano, A., Ardini, F., Grotti, M., Malandrino, M., Giacomino, A., Abollino, O., Cappelletti, D., Becagli, S., Traversi, R., Udisti, R., 2016. Elemental and lead isotopic composition of atmospheric particulate measured in the Arctic region (Ny-Ålesund, Svalbard Islands). Rend. Lincei. 27, 73–84. https://doi.org/10.1007/S12210-016-0507-9.

Becagli, S., Caiazzo, L., Di Iorio, T., di Sarra, A., Meloni, D., Muscari, G., Pace, G., Severi, M., Traversi, R., 2020. New insights on metals in the Arctic aerosol in a climate changing world. Sci. Total Environ. 741 (140511), 1–9. https://doi.org/10.1016/J.SCITOTENV.2020.140511.

Boutron, C., Barbante, C., Hong, S., Rosman, K., Bolshov, M., Adams, F., Gabrielli, P., Plane, J., Hur, S.-D., Ferrari, C., Cescon, P., 2011. Heavy metals in Antarctic and Greenland snow and ice cores: man induced changes during the last millennia and natural variations during the last climatic cycles. Persistent Pollut. – Past, Present Futur. 19–46 https://doi.org/10.1007/978-3-642-17419-3_3.

Candelone, J.P., Jaffrezo, J.L., Hong, S., Davidson, C.I., Boutron, C.F., 1996. Seasonal variations in heavy metals concentrations in present day Greenland snow. Sci. Total Environ. 193, 101–110. https://doi.org/10.1016/S0048-9697(96)05325-9.

Cereceda-Balic, F., Palomo-Marin, M.R., Bernalte, E., Vidal, V., Christie, J., Fadic, X., Guevara, J.L., Miro, C., Pinilla Gil, E., 2012. Impact of Santiago de Chile urban atmospheric pollution on anthropogenic trace elements enrichment in snow precipitation at Cerro Colorado, Central Andes. Atmos. Environ. 47, 51–57.

Chekushin, V.A., Bogatyrev, I.V., de Caritat, P., Niskavaara, H., Reimann, C., 1998. Annual atmospheric deposition of 16 elements in eight catchments of the central Barents region. Sci. Total Environ. 220, 95–114.

Ciais, P., Sabine, C., Bala, G., Bopp, L., Brovkin, V., Canadell, J., Chhabra, A., DeFries, R., Galloway, J., Heimann, M., Jones, C., Le Quéré, C., Myneni, R.B., Piao, S., Thornton, P., 2013. Carbon and other biogeochemical cycles. Climate change 2013: the physical science basis. Contribution of Working Group I to the Fifth Assessment Report of the Intergovernmental Panel on Climate Change. Comput. Geom. 18, 95–123.

Colin, J.L., Lim, B., Herms, E., Genet, F., Drab, E., Jaffrezo, J.L., Davidson, C.I., 1997. Air-to-snow mineral transfer—Crustal elements in aerosols, fresh snow and snowpits on the Greenland Ice Sheet. Atmos. Environ. 31, 3395–3406. https://doi.org/10.1016/S1352-2310(97)00122-2.

Conca, E., Abollino, O., Giacomino, A., Buoso, S., Traversi, R., Becagli, S., Grotti, M., Malandrino, M., 2019. Source identification and temporal evolution of trace elements in PM10 collected near to Ny-Ålesund (Norwegian Arctic). Atmos. Environ. 203, 153–165. https://doi.org/10.1016/J.ATMOSENV.2019.02.001.

Conca, E., Malandrino, M., Giacomino, A., Inaudi, P., Giordano, A., Ardini, F., Traversi, R., Abollino, O., 2021. Chemical fractionation of trace elements in Arctic PM10 samples. Atmos. 12, 1152. https://doi.org/10.3390/ATMOS12091152.

Cuss, C.W., Donner, M.W., Grant-Weaver, I., Noernberg, T., Pelletier, R., Sinnatamby, R. N., Shotyk, W., 2018. Measuring the distribution of trace elements amongst dissolved colloidal species as a fingerprint for the contribution of tributaries to large boreal rivers. Sci. Total Environ. 642, 1242–1251. https://doi.org/10.1016/J.SCITOTENV.2018.06.099.

de Caritat, P., Reimann, C., Chekushin, C., Bogatyrev, I., Niskavaara, H., Braun, J., 1997. Mass balance between emission and deposition of airborne contaminants. Environ. Sci. Technol. 31 (2966–2972), 1997.

de Caritat, P., Äyräs, M., Niskavaara, H., Chekushin, V., Bogatyrev, I., Reimann, C., 1998. Snow composition in eight catchments in the central Barents Euro-Arctic region. Atmos. Environ. 32, 2609–2626.

de Caritat, P., Hall, G., Gislason, S., Belsey, W., Braun, M., Goloubeva, N.I., Olsen, H.K., Scheie, J.O., Vaive, J.E., 2005. Chemical composition of arctic snow: concentration level and regional distribution of major elements. Sci. Total Environ. 336, 183–199.

Deng, L., Zhang, Y., Chen, F., Cao, S., You, S., Liu, Y., Zhang, Y., 2013. Reactive Crystallization of Calcium Sulfate Dihydrate from Acidic Wastewater and Lime. Chin. J. Chem. Eng. 21 (11), 1303–1312. https://doi.org/10.1016/S1004-9541(13)60626-6.

Dong, Z., Kang, S., Qin, X., Li, X., Qin, D., Ren, J., 2015. New insights into trace elements deposition in the snow packs at remote alpine glaciers in the northern Tibetan Plateau, China. Sci. Total Environ. 529, 101–113. https://doi.org/10.1016/J.SCITOTENV.2015.05.065.

Douglas, T.A., Sturm, M., 2004. Arctic haze, mercury and the chemical composition of snow across northwestern Alaska. Atmos. Environ. 38, 805–820. https://doi.org/10.1016/J.ATMOSENV.2003.10.042.

Garbarino, J.R., Snyder-Conn, E., Leiker, T.J., Hoffman, G.L., 2002. Contaminants in arctic snow collected over northwest Alaskan sea ice. Water Air Soil Pollut. 139, 183–214.

Goldstein, A.H., Galbally, I.E., 2007. Known and unexplored organic constituents in the Earth's atmosphere. Environ. Sci. Technol. 1516–1521.

Graber, E.R., Rudich, Y., 2006. Atmospheric HULIS: how humic-like are they? A comprehensive and critical review. Atmos. Chem. Phys. 6 (3), 729–753.

Guéguen, C., Cuss, C.W., Cho, S., 2016. Snowpack deposition of trace elements in the Athabasca oil sands region, Canada. Chemosphere 2016 (153), 447–454.

Guo, L., Santschi, P.H., 2006. Ultrafiltration and its applications to sampling and characterisation of aquatic colloids, in: K.J. Wilkinson and J.R. Lead, Eds. Environmental Colloids and Particles: Behaviour, Separation and Characterisation, 10, 159–221, doi:https://doi.org/10.1002/9780470024539.ch4.

Guo, L., Wen, L.-S., Tang, D., Santschi, P.H., 2000. Re-examination of cross-flow ultrafilration for sampling aquatic colloids: evidence from molecular probes. Mar. Chem. 69, 75–90.

Guo, L., Hunt, B.J., Santschi, P.H., 2001. Ultrafiltration behavior of major ions (Na, Ca, Mg, F, Cl, and SO_4) in natural waters. Water Res. 35 (6), 1500–1508.

Ilina, S.M., Lapitsky, S.A., Alekhin, Y.V., Viers, J., Benedetti, M., Pokrovsky, O.S., 2016. Speciation, size fractionation and transport of trace element in the continuum soil water – mire – lake – river – large oligotrophic lake of a subarctic watershed. Aquat. Geochem. 22 (1), 65–95. https://doi.org/10.1007/s10498-015-9277-8.

Jaffe, D., Cerundolo, B., Rickers, J., Stolzberg, R., Baklanov, A., 1995. Deposition of sulfate and heavy metals on the Kola Peninsula. Sci. Total Environ. 160–161, 127–134. https://doi.org/10.1016/0048-9697(95)04350-A.

Javed, M.B., Cuss, C.W., Zheng, J., Grant-Weaver, I., Noernberg, T., Shotyk, W., 2022. Size-fractionation of trace elements in dusty snow from open pit bitumen mines and upgraders: collection, handling, preparation and analysis of samples from the Athabasca bituminous sands region of Alberta, Canada. Envrion. Sci.: Atmos. 2 https://doi.org/10.1039/d1ea00034a. Art no 428.

Jensen, L.T., Lanning, N.T., Marsay, C.M., Buck, C.S., Aguilar-Islas, A.M., Rember, R., Landing, W.M., Sherrell, R.M., Fitzsimmons, J.N., 2021. Biogeochemical cycling of colloidal trace metals in the Arctic cryosphere. J. Geophys. Res. - Oceans 126 (8). https://doi.org/10.1029/2021JC017394. Art No e2021JC017394.

Jung, J., Hong, S., Chen, M., Hur, J., Jiao, L., Lee, Y., Park, K., Hahm, D., Choi, J.-O., Yang, E.-J., Park, J., Kim, T.-W., Lee, S., 2020. Characteristics of methanesulfonic acid, non-sea-salt sulfate and organic carbon aerosols over the Amundsen Sea, Antarctica. Atmos. Chem. Phys. 20, 5405–5424. https://doi.org/10.5194/acp-20-5405-2020.

Kang, S., Zhang, Q., Kaspari, S., Qin, D., Cong, Z., Ren, J., Mayewski, P.A., 2007. Spatial and seasonal variations of elemental composition in Mt. Everest (Qomolangma) snow/firn. Atmos. Environ. 41, 7208–7218.

Karnatzevicth, I.V., Khruschev, S.A., 2014. A computer system of mass calculation of running water balances of river watersheds from poorly studied territories. Gos. Ped. Institut. 174 (in Russian).

Kashulina, G., de Caritat, P., Reimann, C., 2014. Snow and rain chemistry around the "Severonikel" industrial complex, NW Russia: current status and retrospective analysis. Atmos. Environ. 89, 672–682.
Knopf, D.A., Alpert, P.A., Wang, B., 2018. The role of organic aerosol in atmospheric ice nucleation: a review. ACS Earth Space Chem. 2, 168–202.
Kozak, K., Koziol, K., Luks, B., Chmiel, S., Ruman, M., Marc, M., Namiesnik, J., Polkowska, Z., 2015. The role of atmospheric precipitation in introducing contaminants to the surface waters of the Fuglebekken catchment, Spitsbergen. Polar Res. 34 https://doi.org/10.3402/polar.v34.24207. Art No 24207.
Koziol, K., Uszczyk, A., Pawlak, F., Frankowski, M., Polkowska, Ż., 2021. Seasonal and spatial differences in metal and metalloid concentrations in the snow cover of Hansbreen, Svalbard. Front. Earth Sci. 8, 691. https://doi.org/10.3389/FEART.2020.538762.
Krachler, M., Zheng, J., Koerner, R., Zdanowicz, C., Fisher, D., Shotyk, W., 2005. Increasing atmospheric antimony contamination in the northern hemisphere: snow and ice evidence from Devon Island, Arctic Canada. J. Environ. Monit. 7, 1169–1176.
Krickov, I.V., Pokrovsky, O.S., Manasypov, R.M., Lim, A.G., Shirokova, L.S., Viers, J., 2019. Colloidal transport of carbon and metals by western Siberian rivers during different seasons across a permafrost gradient. Geochim. Cosmochim. Acta 265. https://doi.org/10.1016/j.gca.2019.08.041.
Krickov, I.V., Lim, A.G., Shevchenko, V.P., Vorobyev, S.N., Candaudap, F., Pokrovsky, O. S., 2022. Dissolved metal (Fe, Mn, Zn, Ni, Cu, Co, Cd, Pb) and metalloid (As, Sb) in snow water across a 2800 km latitudinal profile of western siberia: impact of local pollution and global transfer. Water 14, 94. https://doi.org/10.3390/W14010094.
Lai, A.M., Shafer, M.M., Dibb, J.E., Polashenski, C.M., Schauer, J.J., 2017. Elements and inorganic ions as source tracers in recent Greenland snow. Atmos. Environ. 164, 205–215. https://doi.org/10.1016/J.ATMOSENV.2017.05.048.
Lee, S.S., Donner, L.J., Phillips, V.T.J., Ming, Y., 2008. The dependence of aerosol effects on clouds and precipitation on cloud-system organization, shear and stability. J. Geophys. Res. Atmos. 113, 16202. https://doi.org/10.1029/2007JD009224.
Li, Y., Huang, J., Li, Z., Zheng, K., 2020. Atmospheric pollution revealed by trace elements in recent snow from the central to the northern Tibetan Plateau. Environ. Pollut. 263 (Art No 114459).
Lim, S., Lee, M., Rhee, T.S., 2019. Chemical characteristics of submicron aerosols observed at the King Sejong Station in the northern Antarctic Peninsula from fall to spring. Sci. Total Environ. 668, 1310–1316. https://doi.org/10.1016/j.scitotenv.2019.02.099.
Lim, A.G., Loiko, S.V., Pokrovsky, O.S., 2022. Sizable pool of labile organic carbon in peat and mineral soils of permafrost peatlands, western Siberia. Geoderma 409. https://doi.org/10.1016/j.geoderma.2021.115601.
Loiko, S.V., Pokrovsky, O.S., Raudina, T.V., Lim, A., Kolesnichenko, L.G., Shirokova, L.S., Vorobyev, S.N., Kirpotin, S.N., 2017. Abrupt permafrost collapse enhances organic carbon, CO2, nutrient and metal release into surface waters. Chem. Geol. 471, 153–165. https://doi.org/10.1016/j.chemgeo.2017.10.002.
Luo, G., Yu, F., 2010. A numerical evaluation of global oceanic emissions of α-pinene and isoprene. Atmos. Chem. Phys. 10, 2007–2015. https://doi.org/10.5194/acp-10-2007-2010.
Lyvén, B., Hassellöv, M., Turner, D.R., Haraldsson, C., Andersson, K., 2003. Competition between iron- and carbon-based colloidal carriers for trace metals in a freshwater assessed using flow field-flow fractionation coupled to ICPMS. Geochim. Cosmochim. Acta 67, 3791–3802. https://doi.org/10.1016/S0016-7037(03)00087-5.
Ma, X., Gomez, M.A., Yuan, Z., Bi, R., Zhang, J., Wang, S., Yao, S., Kersten, M., Jia, Y., 2020. Incorporation of trace metals Cu, Zn, and Cd into gypsum: Implication on their mobility and fate in natural and anthropogenic environments. Chem. Geol. 541 https://doi.org/10.1016/j.chemgeo.2020.119574. Art No 119574.
Manasypov, R.M., Vorobyev, S.N., Loiko, S.V., Kritzkov, I.V., Shirokova, L.S., Shevchenko, V.P., Kirpotin, S.N., Kulizhsky, S.P., Kolesnichenko, L.G., Zemtzov, V. A., Sinkinov, V.V., Pokrovsky, O.S., 2015. Seasonal dynamics of organic carbon and metals in thermokarst lakes from the discontinuous permafrost zone of western Siberia. Biogeosciences 12. https://doi.org/10.5194/bg-12-3009-2015.
Miler, M., Gosar, M., 2015. Chemical and morphological characteristics of solid metal-bearing phases deposited in snow and stream sediment as indicators of their origin. Environ. Sci. Pollut. Res. 22, 1906–1918. https://doi.org/10.1007/S11356-014-3589-X.
Moskovchenko, D.V., Babushkin, A.G., 2012. Peculiarities of formation of chemical composition of snow waters (on example of Khanty-Mansi autonomous district). Earth Cryosphere XVI, 71–81.
Moskovchenko, D., Pozhitkov, R., Zakharchenko, A., Tigeev, A., 2021. Concentrations of Major and trace elements within the snowpack of Tyumen, Russia. Minerals 11. https://doi.org/10.3390/MIN11070709. Art No 709.
Nichman, L., Wolf, M., Davidovits, P., Onasch, T.B., Zhang, Y., Worsnop, D.R., Bhandari, J., Mazzoleni, C., Cziczo, D.J., 2019. Laboratory study of the heterogeneous ice nucleation on black-carbon-containing aerosol. Atmos. Chem. Phys. 19, 12175–12194. https://doi.org/10.5194/acp-19-12175-2019.
Oleinikova, O.V., Drozdova, O.Y., Lapitskiy, S.A., Demin, V.V., Bychkov, A.Y., Pokrovsky, O.S., 2017. Dissolved organic matter degradation by sunlight coagulates organo-mineral colloids and produces low-molecular weight fraction of metals in boreal humic waters. Geochim. Cosmochim. Acta 211, 97–114. https://doi.org/10.1016/J.GCA.2017.05.023.
Oleinikova, O.V., Shirokova, L.S., Drozdova, O.Y., Lapitskiy, S.A., Pokrovsky, O.S., 2018. Low biodegradability of dissolved organic matter and trace metals from subarctic waters. Sci. Total Environ. 618, 174–187. https://doi.org/10.1016/J.SCITOTENV.2017.10.340.
Payandi-Rolland, D., Shirokova, L.S., Labonne, F., Bénézeth, P., Pokrovsky, O.S., 2021. Impact of freeze-thaw cycles on organic carbon and metals in waters of permafrost peatlands. Chemosphere 279, 130510. https://doi.org/10.1016/J.CHEMOSPHERE.2021.130510.
Pokrovsky, O.S., Schott, J., 2002. Iron colloids/organic matter associated transport of major and trace elements in small boreal rivers and their estuaries (NW Russia). Chem. Geol. 190, 141–179. https://doi.org/10.1016/S0009-2541(02)00115-8.
Pokrovsky, O.S., Viers, J., Shirokova, L.S., Shevchenko, V.P., Filipov, A.S., Dupré, B., 2010. Dissolved, suspended, and colloidal fluxes of organic carbon, major and trace elements in the Severnaya Dvina River and its tributary. Chem. Geol. 273, 136–149. https://doi.org/10.1016/J.CHEMGEO.2010.02.018.
Pokrovsky, O.S., Shirokova, L.S., Zabelina, S.A., Vorobieva, T.Y., Moreva, O.Y., Klimov, S.I., Chupakov, A.V., Shorina, N.V., Kokryatskaya, N.M., Audry, S., Viers, J., Zoutien, C., Freydier, R., 2012. Size fractionation of trace elements in a seasonally stratified boreal lake: Control of organic matter and iron colloids. Aquat. Geochem. 18, 115–139. https://doi.org/10.1007/S10498-011-9154-Z.
Pokrovsky, O.S., Shirokova, L.S., Kirpotin, S.N., 2014. Biogeochemistry of thermokarst lakes of Western Siberia. In: Biogeochemistry of Thermokarst Lakes of Western Siberia. Nova Publishers, N.Y, p. 163.
Pokrovsky, O.S., Manasypov, R.M., Loiko, S.V., Krickov, I.A., Kopysov, S.G., Kolesnichenko, L.G., Vorobyev, S.N., Kirpotin, S.N., 2016a. Trace element transport in western Siberian rivers across a permafrost gradient. Biogeosciences 13, 1877–1900. https://doi.org/10.5194/bg-13-1877-2016.
Pokrovsky, O.S., Manasypov, R.M., Loiko, S.V., Shirokova, L.S., 2016b. Organic and organo-mineral colloids in discontinuous permafrost zone. Geochim. Cosmochim. Acta 188, 1–20. https://doi.org/10.1016/J.GCA.2016.05.035.
Pokrovsky, O.S., Karlsson, J., Giesler, R., 2018. Freeze-thaw cycles of Arctic thaw ponds remove colloidal metals and generate low-molecular-weight organic matter. Biogeochemistry 137, 321–336. https://doi.org/10.1007/S10533-018-0421-6.
Pokrovsky, O.S., Manasypov, R.M., Kopysov, S.G., Krickov, I.V., Shirokova, L.S., Loiko, S. V., Lim, A.G., Kolesnichenko, L.G., Vorobyev, S.N., Kirpotin, S.N., 2020. Impact of permafrost thaw and climate warming on riverine export fluxes of carbon, nutrients and metals in Western Siberia. Water (Switzerland) 2020 (6), 12. https://doi.org/10.3390/w12061817.
Pokrovsky, O., Krickov, I., Shevchenko, V., Vorobyev, S., Lim, A., 2022. Major and trace elements in snow water of Western Siberia. Mendeley Data V1. https://data.mendeley.com/datasets/3vnfk6s9tb.
Pozhitkov, R., Moskovchenko, D., Soromotin, A., Kudryavtsev, A., Tomilova, E., 2020. Trace elements composition of surface snow in the polar zone of northwestern Siberia: the impact of urban and industrial emissions. Environ. Monit. Assess. 192, 1–14. https://doi.org/10.1007/S10661-020-8179-4.
Rankin, A.M., Auld, V., Wolff, E.W., 2000. Frost flowers as a source of fractionated sea salt aerosol in the polar regions. Geophys. Res. Lett. 27 (21), 3469–3472. https://doi.org/10.1029/2000GL011771.
Raudina, T.V., Loiko, S.V., Kuzmina, D.M., Shirokova, L.S., Kulizhskiy, S.P., Golovatskaya, E.A., Pokrovsky, O.S., 2021. Colloidal organic carbon and trace elements in peat porewaters across a permafrost gradient in Western Siberia. Geoderma 390, 114971. https://doi.org/10.1016/j.geoderma.2021.114971.
Reimann, C., Niskavaara, H., de Caritat, P., Finne, T.E., Äyräs, M., Chekushin, V., 1996. Regional variation of snow pack chemistry in the vicinity of Nikel and Zapoljarnij, Russia, northern Finland and Norway. Sci. Total Environ. 182, 147–158.
Reinosdotter, K., Viklander, M., 2005. A comparison of snow quality in two Swedish municipalties – Luleå and Sundsvall. Water Air Soil Pollut. 167, 3–16.
Russel, W.B., Saville, D.A., Schowalter, W.R., 1989. Colloidal Dispersions. Cambridge University Press, Cambridge, UK, p. 506.
Rysgaard, S., Søgaard, D.H., Cooper, M., Pú Cko, M., Lennert, K., Papakyriakou, T.N., Wang, F., Geilfus, N.X., Glud, R.N., Ehn, J., Mcginnnis, D.F., Attard, K., Sievers, J., Deming, J.W., Barber, D., 2013. Ikaite crystal distribution in Arctic winter sea ice. Cryosphere 7, 707–718. https://doi.org/10.5194/tc-7-707-2013.
Salo, K., Zetterdahl, M., Johnson, H., Svensson, E., Magnusson, M., Gabrielii, C., Brynolf, S., 2016. Emissions to the air. Shipp. Environ. Improv. Environ. Perform. Mar. Transp. 169–227 https://doi.org/10.1007/978-3-662-49045-7_5.
Schuur, E.A.G., McGuire, A.D., Schädel, C., Grosse, G., Harden, J.W., Hayes, D.J., Hugelius, G., Koven, C.D., Kuhry, P., Lawrence, D.M., Natali, S.M., Olefeldt, D., Romanovsky, V.E., Schaefer, K., Turetsky, M.R., Treat, C.C., Vonk, J.E., 2015. Climate change and the permafrost carbon feedback. Nature 520 (7546), 171–179. https://doi.org/10.1038/nature14338.
Shaw, G.E., Shaw, J.A., Shaw, R.A., 1993. The snows of interior Alaska. Atmos. Environ. Part A 27, 2091–2096. https://doi.org/10.1016/0960-1686(93)90281-3.
Shevchenko, V.P., Vinogradova, A.A., Lisitzin, A.P., Novigatsky, A.N., Panchenko, M.V., Pol'kin, V.V., 2016. Aeolian and Ice Transport of Matter (Including Pollutants) in the Arctic 59–73. https://doi.org/10.1007/978-3-642-12315-3_5.
Shevchenko, V.P., Pokrovsky, O.S., Vorobyev, S.N., Krickov, I.V., Manasypov, R.M., Politova, N.V., Kopysov, S.G., Dara, O.M., Auda, Y., Shirokova, L.S., Kolesnichenko, L.G., Zemtsov, V.A., Kirpotin, S.N., 2017. Impact of snow deposition on major and trace element concentrations and elementary fluxes in surface waters of the Western Siberian Lowland across a 1700'km latitudinal gradient. Hydrol. Earth Syst. Sci. 21, 5725–5746. https://doi.org/10.5194/HESS-21-5725-2017.
Shirokova, L.S., Pokrovsky, O.S., Kirpotin, S.N., Desmukh, C., Pokrovsky, B.G., Audry, S., Viers, J., 2013. Biogeochemistry of organic carbon, CO_2, CH_4, and trace elements in thermokarst water bodies in discontinuous permafrost zones of Western Siberia. Biogeochemistry 113, 573–593. https://doi.org/10.1007/s10533-012-9790-4.
Snyder-Conn, E., Garbarino, J.R., Hoffman, G.L., Oelkers, A., 1997. Soluble trace elements and total mercury in Arctic Alaskan snow. Arctic 50, 201–215.
Stolpe, B., Guo, L., Shiller, A.M., Aiken, G.R., 2013. Abundance, size distributions and trace-element binding of organic and iron-rich nanocolloids in Alaskan rivers, as

revealed by field-flow fractionation and ICP-MS. Geochim. Cosmochim. Acta 105, 221–239. https://doi.org/10.1016/J.GCA.2012.11.018.

Talovskaya, A.V., Simonenkov, D.V., Filimonenko, E.A., Belan, B.D., Yazikov, E.G., Rychkova, D.A., Il'enok, S.S., 2014. Study of aerosol composition in Tomsk region background and urban stations (the winter period 2012/13). Optika Atmosfery i Okeana 27, 999–1005 (in Russian).

Tamocai, C., Canadell, J.G., Schuur, E.A.G., Kuhry, P., Mazhitova, G., Zimov, S., 2009. Soil organic carbon pools in the northern circumpolar permafrost region. Glob. Biogeochem. Cycles 23, GB2023. https://doi.org/10.1029/2008GB003327.

Telmer, K., Bonham-Carter, G.F., Kliza, D.A., Hall, G.E.M., 2004. The atmospheric transport and deposition of smelter emissions: evidence from the multi-element geochemistry of snow, Quebec, Canada. Geochim. Cosmochim. Acta 2004 (68), 2961–2980.

Thakur, R.C., Thamban, M., 2019. Influence of gaseous and particulate species on neutralization processes of polar aerosol and snow-a case study from Ny-Alesund. J. Environ. Sci. 76, 12–25. https://doi.org/10.1016/j.jes.2018.03.002.

Topchaya, V.Yu., Chechko, V.A., Shevchenko, V.P., 2012. The composition of aeolian material contained in the snow cover of coastal South-Eastern Baltic Sea. Optika Atmospheri i Okeana 25, 518–522 (in Russian).

Tranter, M., Brimblecombe, P., Davies, T.D., Vincent, C.E., Abrahams, P.W., Blackwood, I., 1986. The composition of snowfall, snowpack and meltwater in the Scottish highlands-evidence for preferential elution. Atmos. Environ. 20, 517–525. https://doi.org/10.1016/0004-6981(86)90092-2.

Udachin, V.N., 2012. Ecogeochemistry of the Southern Urals Mining Industry. Doctor of Sciences Thesis. Tomsk Polytechnic University, Tomsk, p. 354 (in Russian).

van Olphen, H., 1977. An Introduction to Clay Colloid Chemistry. John Wiley & Sons.

Vlasov, D., Vasil'chuk, J., Kosheleva, N., Kasimov, N., 2020. Dissolved and Suspended Forms of Metals and Metalloids in Snow Cover of Megacity: Partitioning and Deposition rates in Western Moscow. Atmos. 11, 907. https://doi.org/10.3390/ATMOS11090907.

Walker, T.R., Young, S.D., Crittenden, P.D., Zhang, H., 2003. Anthropogenic metal enrichment of snow and soil in north-eastern European Russia. Environ. Pollut. 121, 11–21.

Wang, X., Pu, W., Zhang, X., Ren, Y., Huang, J., 2015. Water-soluble ions and trace elements in surface snow and their potential source regions across northeastern China. Atmos. Environ. 114, 57–65. https://doi.org/10.1016/J.ATMOSENV.2015.05.012.

Wei, T., Dong, Z., Kang, S., Zong, C., Rostami, M., Shao, Y., 2019. Atmospheric deposition and contamination of trace elements in snowpacks of mountain glaciers in the northeastern Tibetan Plateau. Sci. Total Environ. 689, 754–764.

Xu, H., Guo, L., 2017. Molecular size-dependent abundance and composition of dissolved organic matter in river, lake and sea waters. Water Res. 117, 115–126.

Xu, L., Williams, L.R., Young, D.E., Allan, J.D., Coe, H., Massoli, P., Fortner, E., Chhabra, P., Herndon, S., Brooks, W.A., Jayne, J.T., Worsnop, D.R., Aiken, A.C., Liu, S., Gorkowski, K., Dubey, M.K., Fleming, Z.L., Visser, S., Prévôt, A.S.H., Ng, N.L., 2016. Wintertime aerosol chemical composition, volatility, and spatial variability in the greater London area. Atmos. Chem. Phys. 16, 1139–1160. https://doi.org/10.5194/ACP-16-1139-2016.

Yeghicheyan, D., Aubert, D., Bouhnik-Le Coz, M., Chmeleff, J., Delpoux, Cloquet, C., Marquet, A., Menniti, C., Pradoux, C., Freydier, R., Vieira da Silva-Filho, E., Suchorski, K., 2019. A new interlaboratory characterisation of silicon, rare earth elements and twenty two other trace element mass fractions in the natural river water Certified Reference Material SLRS -6 (NRC - CNRC). Geostand. Geoanal. Res. 43 (3), 475–496. https://doi.org/10.1111/J.1751-908X.2013.00232.X.